Journal of Volcanology and Geothermal Research 391 (2020) 106435

Contents lists available at ScienceDirect

Journal of Volcanology and Geothermal Research

journal homepage: www.elsevier.com/locate/jvolgeores

The Iceland Deep Drilling Project at Reykjanes: Drilling into the root zone of a black smoker analog

Guðmundur Ó. Friðleifsson [a,*], Wilfred A. Elders [b], Robert A. Zierenberg [c], Andrew P.G. Fowler [d], Tobias B. Weisenberger [e], Kiflom G. Mesfin [a], Ómar Sigurðsson [a], Steinþór Níelsson [e], Gunnlaugur Einarsson [e], Finnbogi Óskarsson [e], Egill Á. Guðnason [e], Helga Tulinius [e], Ketil Hokstad [f], Gibert Benoit [g], Frank Nono [g,h], Didier Loggia [g], Fleurice Parat [g], Sarah B. Cichy [g,i], David Escobedo [g], David Mainprice [g]

[a] HS Orka, Svartsengi, 240 Grindavík, Iceland
[b] Dept. of Earth Sciences, University of California, Riverside, CA 92521, USA
[c] Dept. of Earth and Planetary Sciences, University of California, Davis, CA 95616, USA
[d] Department of Earth Sciences, University of Minnesota, Minneapolis, USA
[e] ÍSOR, Grensásvegur 9, 108 Reykjavík, Iceland
[f] Statoil Research Centre, Trondheim, Norway
[g] Géosciences Montpellier, Université de Montpellier, France
[h] Université de Pau, France
[i] University of Potsdam and GFZ, Potsdam, Germany

A R T I C L E I N F O

Article history:
Received 28 November 2017
Received in revised form 24 May 2018
Accepted 23 August 2018
Available online 31 August 2018

Keywords:
IDDP
Reykjanes
Supercritical fluids
Deep drilling
Black smokers
Geothermal

A B S T R A C T

The aim of the Iceland Deep Drilling Project is to drill into supercritical geothermal systems and examine their economic potential. The exploratory well IDDP-2 was drilled in the Reykjanes geothermal field in SW Iceland, on the landward extension of the Mid-Atlantic Ridge. The Reykjanes geothermal field produces from a <300 °C reservoir at 1 to 2.5 km depth and is unusual because it is recharged by seawater. The well was cased to 3000 m depth, and then angled towards the main up-flow zone of the system, to a total slant depth of 4659 m (~4500 m vertical depth). Based on alteration mineral assemblages, joint inversion of wireline logging, and rate of heating measurements, the bottom hole temperature is estimated to be about 535 °C.

The major problem encountered during drilling was the total loss of circulation below 3 km depth and continuing to the final depth. Drilling continued without recovering drill cuttings, consequently spot coring provided the only deep rock samples from the well. These cores are characteristic of a basaltic sheeted dike complex, with hydrothermal alteration mineral assemblages that range from greenschist to amphibolite facies, hornblende hornfels, and pyroxene hornfels, allowing the opportunity to investigate water-rock interaction in the active roots of an analog of a submarine hydrothermal system. As they have not yet been sampled, the composition of the deep fluids at Reykjanes is unknown at present. Cold water is currently being injected with the aim of enhancing permeability at depth, before allowing the well to heat up prior to flow tests planned for early 2019. The well has at least two fluid feed zones, a dominant one at 3.4 km depth and a second smaller one at 4.5 km.

Extensive geophysical surveys of the Reykjanes Peninsula completed recently allow correlation of geophysical signals with rocks properties and in-situ conditions in the subsurface. Earthquake activity monitored with a local seismic network during drilling the IDDP-2 drilling detected abundant small earthquakes ($M_L \le 2$) within the depth range of 3–5 km. A zone at 3–5 km depth below the producing geothermal field that was generally aseismic prior to drilling, but became seismically active during the drilling.

The drilling of the IDDP-2 has achieved number of scientific and engineering firsts. It is the deepest and hottest drill hole so far sited on an active mid-ocean spreading center. It penetrated an active supercritical hydrothermal environment at depths analogous to those postulated as the high temperature reaction zones feeding black smoker systems.

1. Introduction

The aim of the Iceland Deep Drilling Project (IDDP) is to explore the feasibility, technology, and economics of producing supercritical

* Corresponding author.
E-mail address: gof@hsorka.is (G.Ó. Friðleifsson).

https://doi.org/10.1016/j.jvolgeores.2018.08.013

geothermal resources. The IDDP-2 well was recently completed at Reykjanes in SW-Iceland on the landward extension of the Mid-Atlantic Ridge (Fig. 1), and the project was successful in reaching its immediate objective of demonstrating that it is possible to drill a supercritical geothermal well (Friðleifsson and Elders, 2017; Friðleifsson et al., 2017). Flow tests are planned for 2019 to determine the potential energy output of the well where we hope to demonstrate that a new, potentially very large and more economic geothermal resource will become available. This paper provides an overview of the motivation and background of the IDDP, describes new results from, and future plans for the IDDP-2 well, and discusses both its scientific and geothermal implications.

Iceland is the largest land mass astride an oceanic spreading center because it also is the surface expression of a mantle hotspot that produces a very high flux of basaltic magma (Fig. 1). High temperature reactions between seawater and basalt at Reykjanes provide a unique opportunity to explore physical conditions that control hydrothermal fluid composition in the roots of submarine black smoker systems that occur along much of mid-ocean ridge spreading systems, including the Reykjanes Ridge. (Palgan et al., 2017). The chemical composition of the Reykjanes geothermal fluids is similar to those of black smokers and the fluids precipitate base-metal sulfide deposits similar to black smoker chimneys (Harðardóttir et al., 2012, 2013). The most significant difference between typical black smoker vents and the Reykjanes geothermal system is the pressure difference at the surface, which results in subsurface boiling and deposition of metals at Reykjanes in contrast to chimney formation by cooling during mixing with seawater on the seafloor. A more important comparison is to the temperature and pressure conditions at which high temperature water-rock reaction sets the composition of the geothermal fluids. Our drilling results confirm that supercritical temperatures are attained below Reykjanes at pressures and depths below sea level comparable to the base of the sheeted dike

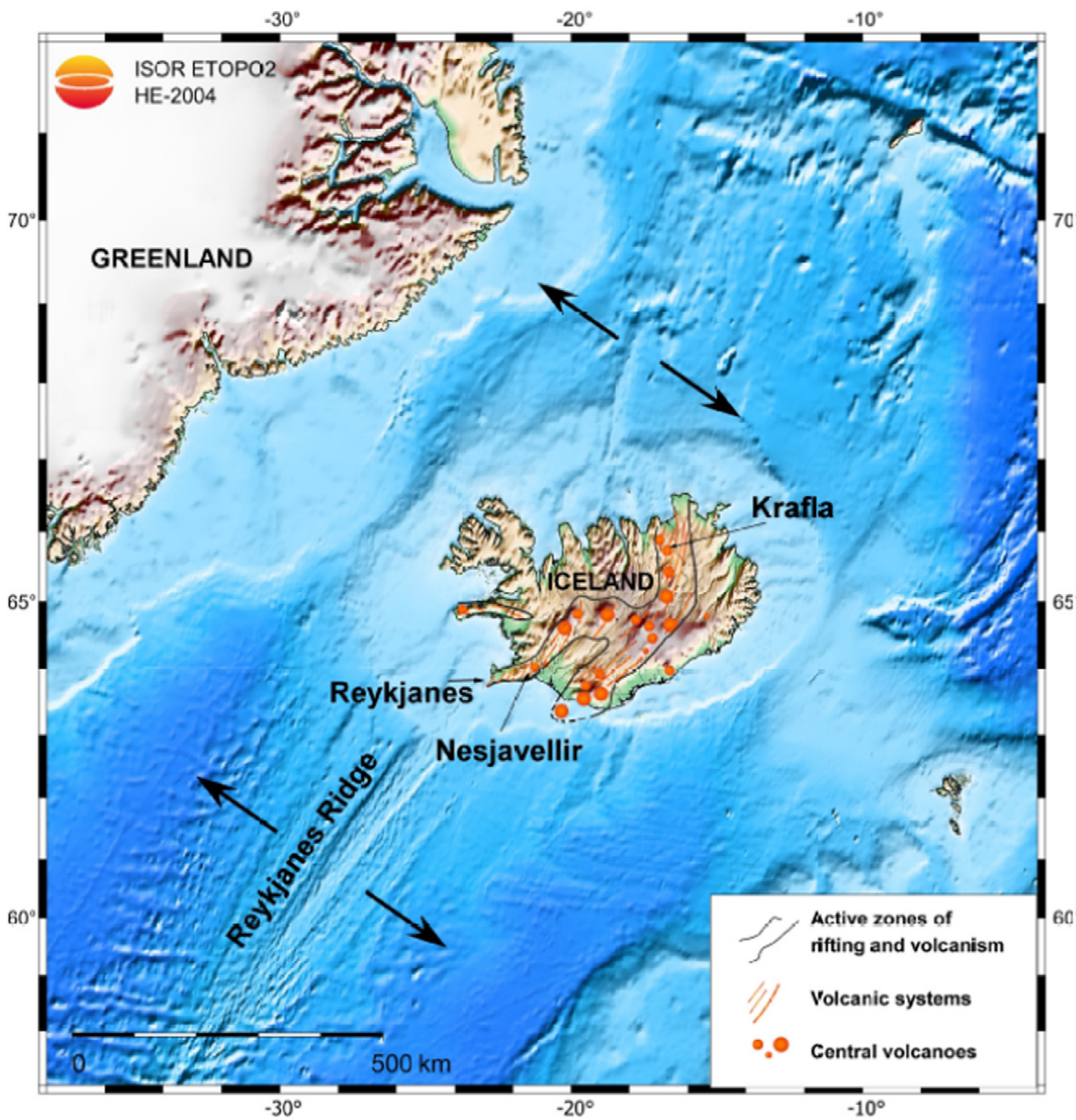

Fig. 1. The location of Iceland on the Mid-Atlantic Ridge. The arrows show the spreading directions on the Reykjanes ridge to the south and the Kolbeinsey Ridge to the north. Iceland's neovolcanic zone with its active central volcanoes hosts the three high temperature systems of Reykjanes, Nesjavellir (in the Hengill Volcano), and Krafla, that were chosen as suitable for IDDP deep drilling.

section below typical MOR vent systems. The IDDP-2 is therefore able to explore the roots of a black smoker analog without the technical challenges that have precluded seafloor drilling into this scientifically significant environment.

A major milestone for the IDDP was completion of well IDDP-2 at Reykjanes on January 25, 2017 to a slant depth of 4659 m from the rig floor (Weisenberger et al., 2017). The upper part of the well is vertical (Jónsson et al., 2010) but it was directionally drilled to the southwest from about 2750 m to the final depth. The true vertical depth from ground surface is close to 4500 m. This appears to be the first geothermal production well worldwide to successfully reach supercritical conditions. Some preliminary results from IDDP-2 have already been described in several conference reports and papers (e.g. Friðleifsson and Elders, 2017; Friðleifsson et al., 2017; Zierenberg et al., 2017; Stefánsson et al., 2017; Hokstad and Tänavsuu-Milkeviciene, 2017).

The Iceland Deep Drilling Project (IDDP) was organized and funded by a consortium consisting of three Icelandic energy companies (HS Orka, Landsvirkjun and Orkuveita Reykjavíkur), together with Orkustofnun (the Energy Authority of Iceland), and later with additional funding from Statoil. The idea of deep drilling to reach supercritical conditions was introduced at the 2000 World Geothermal Congress where it attracted interest from the international geothermal and scientific community (Friðleifsson and Albertsson, 2000; Elders et al., 2001). A three-part IDDP Feasibility Report was produced in 2003, outlining Geoscience Objectives and Site Selection criteria (Friðleifsson et al., 2003), Drilling Technology (Thórhallsson et al., 2003), and Fluid Handling and Evaluation (Albertsson et al., 2003). Modeling studies suggest that producing superheated steam from a hydrothermal reservoir with temperatures > 450 °C could increase power output of a geothermal well by an order of magnitude compared to that produced from a 300 °C geothermal reservoir (Albertsson et al., 2003; Friðleifsson and Elders, 2005; Tester, 2006).

2. Supercritical geothermal resources

The critical point for pure water, where the distinction between liquid, vapor, and steam disappears, is at 374 °C and 22.1 MPa (Fig. 2A). The aim of the IDDP is to access supercritical fluids with high enthalpy that, on flowing upwards, decompress to superheated steam. Not only do such fluids have higher enthalpy than conventional geothermal fluids, but they also exhibit extremely high rates of mass transport due to the greatly enhanced ratios of buoyancy forces to viscous forces in the supercritical state (Dunn and Hardee, 1981; Fournier, 1999, 2007; Yano and Ishido, 1998).

To drill into a hydrothermal system where both temperature and pressure are greater than the critical point not only requires reaching the relevant temperatures, but also hydrostatic pressures found at greater depths than 4 to 5 km.

As indicated in Fig. 2A, dissolved salts or gases affect the critical point of water, so that, for example, the critical point for seawater is at 406 °C and 29.8 MPa (Bischoff and Rosenbauer, 1988). This is relevant to the IDDP-2 as the production fluid from the Reykjanes geothermal field is seawater modified by reactions with basalt at high-temperatures.

In Fig. 2B, the brown shaded area represents the pressure-enthalpy regime found in the geothermal reservoir feeding the existing production wells at Reykjanes. The phase boundaries shown are for pure water, whereas the critical point for Reykjanes fluids which have 3.5% salt, approximates seawater. Before the IDDP-2 was drilled, Friðriksson et al. (2015) considered possible fluid scenarios for the well, depending on the pressure/temperature regime encountered at depth. Three different methods to estimate the temperature at 5 km depth yielded 382 °C, 441 °C and 550 °C (1, 2 and 3 in Fig. 2B). In each case the source fluid was assumed to be in equilibrium with quartz. For simplicity other fluid-mineral equilibria were disregarded. The three models resulted in very different fluids with different production properties; the first being subcritical single-phase fluid similar to the currently produced fluids in Reykjanes, only hotter and with higher silica scaling potential; the second is either superheated steam or a mixture of low salinity vapor (<3.5 wt%) and brine, similar to what has been observed in some ocean-floor black smokers (Coumou et al., 2009); and the third case is superheated steam similar to what was observed in IDDP-1 (Ármannsson et al., 2014), which has significant concentrations of silica and HCl. Given the temperature gradients anticipated in the IDDP-2, cases 2 and 3 appeared to be most applicable, and both would have enlarged potential for silica scaling.

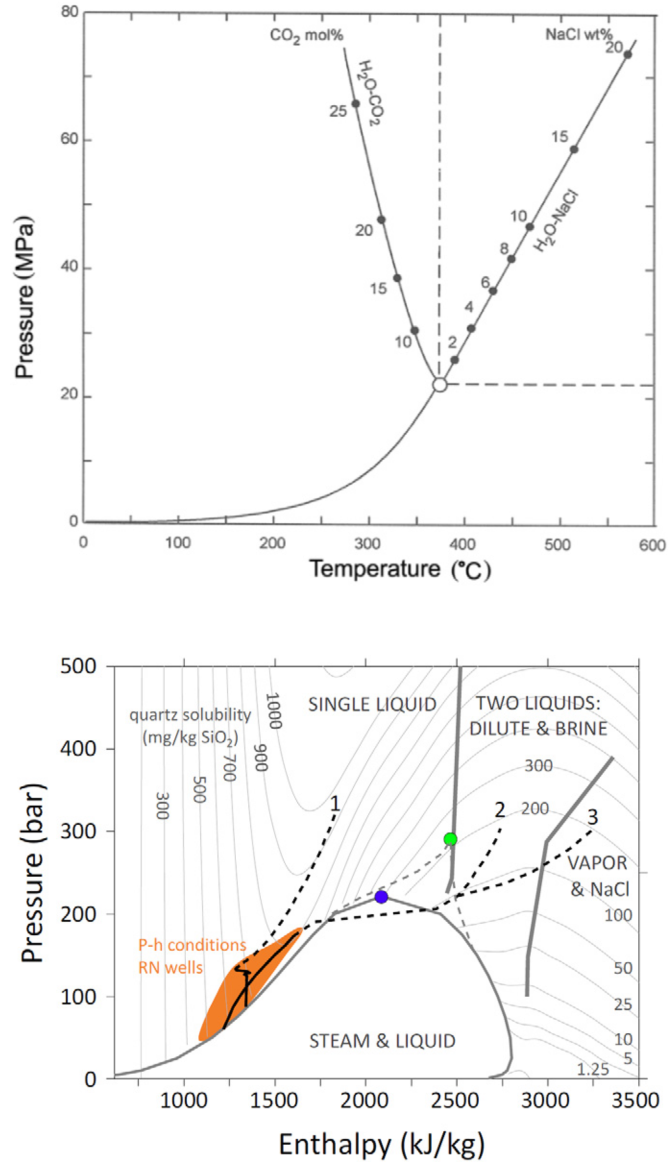

Fig. 2. A. The boiling point curve and critical point curves for water. The critical point for pure water is indicated by the open circle at 374 °C and 22.1 MPa. As shown by the relevant critical point curves for H_2O-NaCl and H_2O-CO_2, dissolved salt increases the temperature and pressure of the critical point whereas dissolved gas reduces the temperature and elevates the pressure of the critical point (Hashida et al., 2001). B. Phase diagram for H_2O in terms of pressure and enthalpy with superimposed quartz solubility (gray contour lines). The labeled phase fields are for pure water. The phase fields for a 3.5% NaCl-H2O system (single liquid, dilute fluid/brine, and vapor/solid NaCl), would have similar shape and pass through the critical point for seawater (green point). The P-h conditions at the three scenarios considered by Friðriksson et al. (2015) are labeled 1, 2 and 3. The critical points for pure water and seawater are shown by blue and green symbols, respectively.

3. The IDDP-1

In 2005 a plan for drilling the first IDDP well at Reykjanes was proposed by deepening RN-17, an existing production well, to a depth of 4–5 km to make certain of reaching a supercritical environment (Fig. 3). The Reykjanes geothermal field is unique in Iceland in that, because it is situated on a narrow peninsula, seawater recharges its reservoir and is the medium of pressure regulation. However, this plan could not be realized. Before deepening could begin, the uncased 3 km deep well collapsed during a flow test, and unfortunately attempts in 2006 to recondition RN-17 for deepening failed. For various reasons IDDP then moved to the Krafla caldera, in NE Iceland, to drill the IDDP-1, in 2008–2009. Given the geothermal gradients known to depths of ~2 km at Krafla, supercritical conditions should exist at 4–5 km depths. This attempt at drilling to supercritical in the IDDP-1 was unsuccessful as the borehole penetrated a nearly aphyric rhyolite magma at >900 °C, at only 2100 m depth, but with fluid pressures well below the critical point of the low salinity meteoric water-sourced fluids (Elders et al., 2011; Zierenberg et al., 2012). The IDDP-1 was completed with a slotted production liner set above the rhyolite magma, where there was good permeability. In subsequent long-term flow tests, IDDP produced superheated steam with a wellhead temperature of 452 °C at a flow rate and enthalpy sufficient to generate about 35 MWe. When flowing this was the world's hottest production well, but, after two years of successful production tests, repair of the surface installations became necessary, resulting in the need to quench the well. This caused collapse of the well casing and ultimately abandonment of the well. The IDDP-1 well is described in 14 papers in a special issue of Geothermics, volume 49, 2014, accessible through Science Direct (http://iddp.is/2014/01/15/geothermics-special-issue-on-iddp-january-2014/).

4. The Reykjanes geothermal field

The field operator Hitaveita Suðurnesja (now HS Orka), drilled its first well in 1999 followed by 15 additional wells before commissioning a 100 MWe power plant in 2006. Since then, ten more wells have been

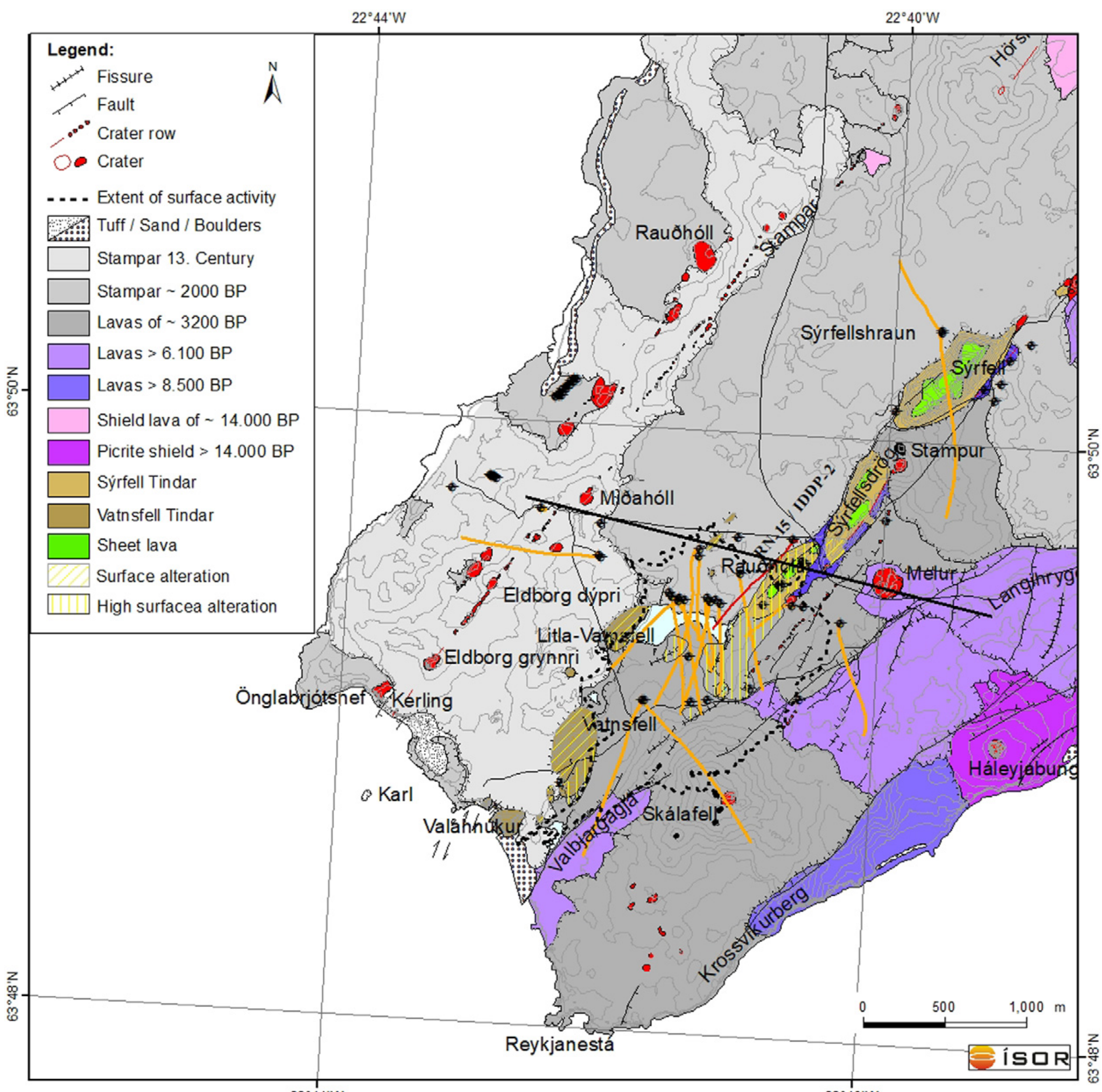

Fig. 3. Geologic map showing the location of all drill holes (circled crosses). The orange colored lines show the direction of inclined wells. Most of the geothermal wells are located within the hydrothermally active field (thin dashed black line), while reinjection wells, some exploration wells and most of the shallow water wells are outside of this area. The youngest eruptive fissures (red colored irregular shaped features) and lavas are located west of the surface expression of hydrothermal activity. The black line running from Miðahóll to Melur shows the location of cross section in Fig. 5.

added, including 2 re-injection wells (RN-33 and RN-34), and 2 step-out wells (RN-29 and RN-30). In July 2017, the drilling of RN-35, a make-up well, began and was completed by the end of September at a slant depth of 2791 m depth. A step out well, RN-36, was then completed in March 2018, at a slant depth of 2381 m.

The wells provide constraints on the subsurface geological and geophysical conditions of the geothermal field. The locations of all wells at Reykjanes are shown on the geological map in Fig. 3. Reports, are available for each of the wells drilled in the past 20 years. These include the drilling operations, flow testing results, downhole P-T logging, wellhead fluid sampling and chemical monitoring. Much of these data are incorporated into a Petrel model at ISOR (the Iceland Geosurvey). Figs. 3, 4, and 5 are selected from that database, showing the surface geology (Fig. 3), temperature profiles with depth, (Fig. 4) and a cross section showing the hydrothermal alteration pattern (Fig. 5). While some of this information may be upgraded with time (e.g. earthquakes in different periods and fluid chemistry), other data have more permanent value (e.g. hydrothermal alteration zonation and subsurface lithology).

A detailed report on the surface geology and the structural characteristics of the Reykjanes area are presented in another contribution submitted to this volume (Saemundsson et al., 2018). In brief, the hydrothermal up-flow zone and surface hydrothermal activity at Reykjanes is centered within the late glacial hyaloclastite ridges (Tindar in Fig. 3) and early Holocene eruptive fissures (Fig. 3). The subsurface lithology to about 2.5 km depth in the Reykjanes field has been described in numerous contributions (e.g. Björnsson et al., 1972; Franzson et al., 2002; Friðleifsson et al., 2003, 2014; Marks et al., 2010). The lithology down to about 2 km depth is characterized by subglacial and submarine hyaloclastite tuffs and sediments at shallower levels, and pillow basalts and breccias at deeper levels. Below about 1.5 km depth the intrusive rock intensity, in the form of basaltic dikes and sheets, increases dramatically in some wells, while pillow basalts and shallow marine deposits are found at depths in others, e.g. in spot cores from RN-17B. The presence of shallow marine deposits at depth records the subsidence of the central part of the rift zone. Friðleifsson and Richter (2010) estimated the average subsidence rate of the Reykjanes strata to about 6 mm/year for half a million years, which is comparable with Vadon and Sigmundsson's (1997) calculations from Satellite Radar Interferometry over a 3 years period 1992–1995. Subsidence and rifting are continuing as evidenced by major (>M5) seismic events, that occur at intervals of several decades, and by the presence of Holocene normal faults with throws of several tens of meters (Saemundsson et al., 2018). The major seismic events affect both the hydrothermal field and its overlying fumaroles. Apparently, this seismic activity temporarily enhances fracture permeability within the reservoir.

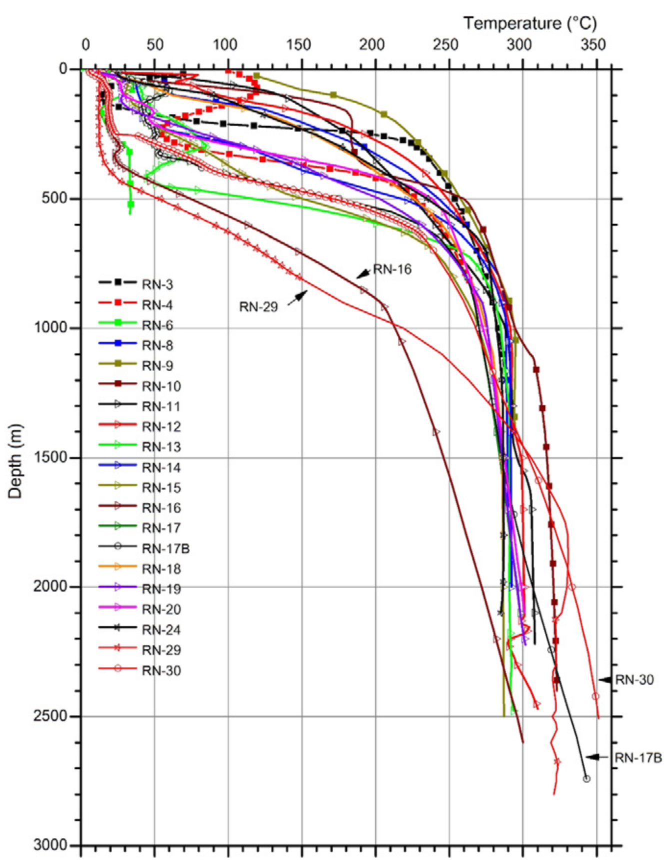

Fig. 4. Steady state temperature-depth profiles for most of the Reykjanes wells, showing the convective temperature distribution with increasing depth that characterizes wells within the currently producing up-flow zone of the Reykjanes geothermal system.

These temperature profiles provide insight into fluid convection in the currently producing upper portion of the Reykjanes hydrothermal system down to about 2.5 km, below the original water table (located at 400–500 m depth). Exceptions are temperature profiles in two wells located outside and to the west of the main up-flow zone, wells RN-16 and RN-29. RN-16 has a conductive character to the base, and RN-29 the temperatures increase conductively to about 1.5 km but show convective behavior deeper in the well. Temperature profiles for wells RN-17B and RN-30 indicate fluid convection within the production field, and conductive heating in the lowermost 1 km of the wells (Fig. 4). The lowermost 1 km of RN-17B and RN-30 extend outside of the main up-flow zone southwards and southeastward, respectively (Fig. 3).

Fig. 5 is a cross section across the middle of the Reykjanes well field based on drill hole and geophysical data. The resistivity model used is from Karlsdóttir et al. (2012). Wells RN-29 and RN-16 are furthest to the left (west) in this section, while most productive wells cluster in the center of the cross section. The inclined well IDDP-2 (colored pink) enters the field of view below 3 km depth, stretching down to about 4.5 km depth, inside a lower resistivity (green colored) field which is surrounded by higher resistivity (blue colored) resistivity field. The lower resistivity green column, targeted by the IDDP-2 well, is interpreted as a hotter, and apparently more permeable, up-flow zone lying below the overlying production field, shown by lighter green, yellow and red resistivity regions of lower resistivity. Three paleo temperature surfaces are defined by connecting the first appearance of hydrothermal alteration index minerals between wells, which rise to the shallowest depths within the center of the well field (Fig. 5). The hydrothermal index minerals are quartz, epidote and actinolite, which precipitate in voids and fractures from geothermal fluids at temperatures above 180 °C, 230 °C and 280 °C respectively (Kristmannsdóttir, 1979).

5. Fluid chemistry of the Reykjanes system

The geothermal fluid in the Reykjanes geothermal system is derived from the heating of cold seawater, modified by reactions with basalt and the precipitation of alteration minerals, and possible additions of magmatic gases from intrusions beneath the geothermal reservoir (Arnórsson, 1978). The pre-production chloride content of the reservoir fluid matches that of local seawater (19,200 mg/kg; Fig. 6), and sodium is near seawater concentrations, although some Na is lost to albitization of feldspars. Important deviations from seawater composition for other non-volatiles include increased concentrations of silica, potassium, and calcium, all of which can be explained by basalt dissolution and equilibria with secondary minerals. There are also decreased concentrations of sulfate and magnesium due to precipitation of secondary minerals such as anhydrite and magnesium phyllosilicates (Arnórsson, 1978).

Elevated concentrations of CO_2 and other volatiles relative to seawater can be attributed to basalt dissolution and direct input from cooling intrusions below the geothermal reservoir. The concentration of the

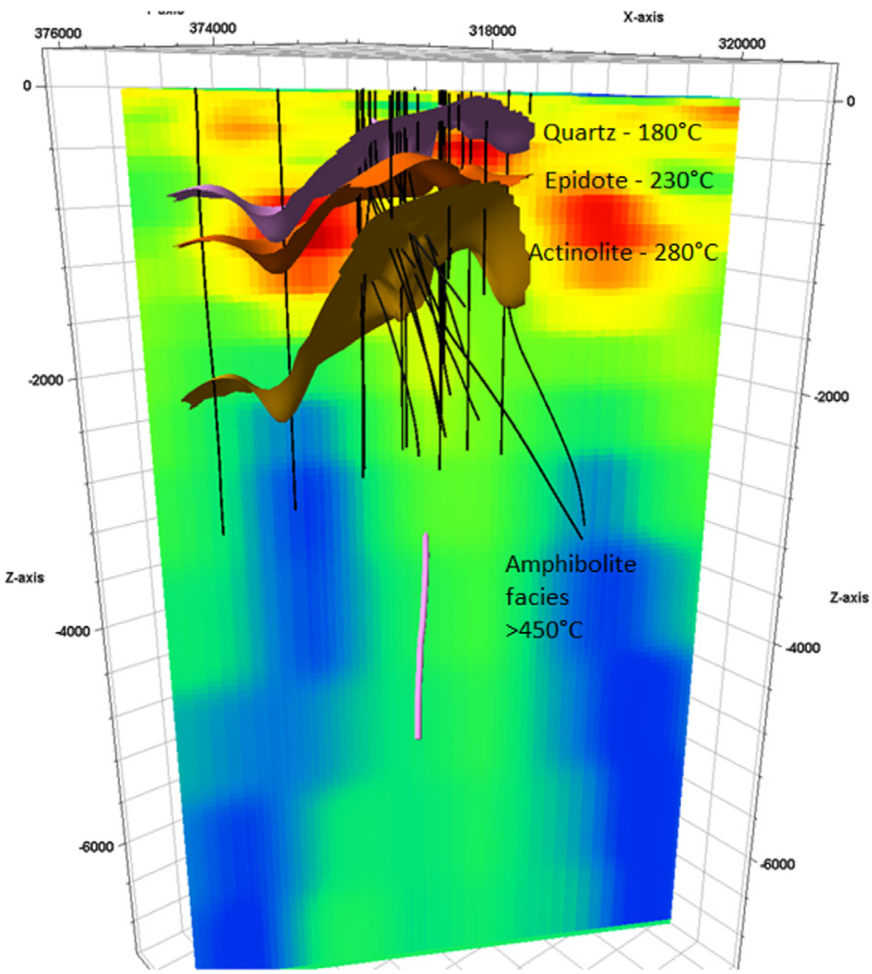

Fig. 5. A WNW-ESE cross section across the middle of the up-flow zone extracted from a 3D resistivity model. Location of cross section line shown in Fig. 3. Well RN-15/DDP-2 (colored pink) is within the field of view below about 3200 m and extends down to the total depth shown in the section. Surfaces interpolated between wells based on the first appearance of hydrothermal quartz (purple), epidote (orange) and actinolite (brown) are shown and have the minimum depths within the center of the well field.

semi-volatile element boron is also higher in the Reykjanes well fluids than in seawater.

Fig. 7 shows the reservoir chloride concentration plotted against the concentration of boron, along with lines representing the average Cl/B ratio in the Reykjanes fluids, local seawater (Cl/B mass ratio 4510; Bjarnason, 1995), and Icelandic basalt (Cl/B molal ratio in tholeiites 25–50; Arnórsson and Andrésdóttir, 1995).

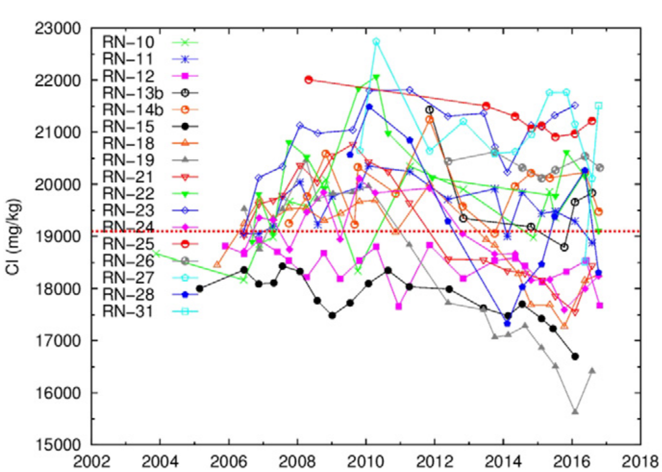

Fig. 6. Concentration of chloride in the reservoir fluid, 2003–2016 produced by various Reykjanes wells. The Cl concentration in local coastal seawater is given by the red dashed line. From Óskarsson and Gałeczka (2017).

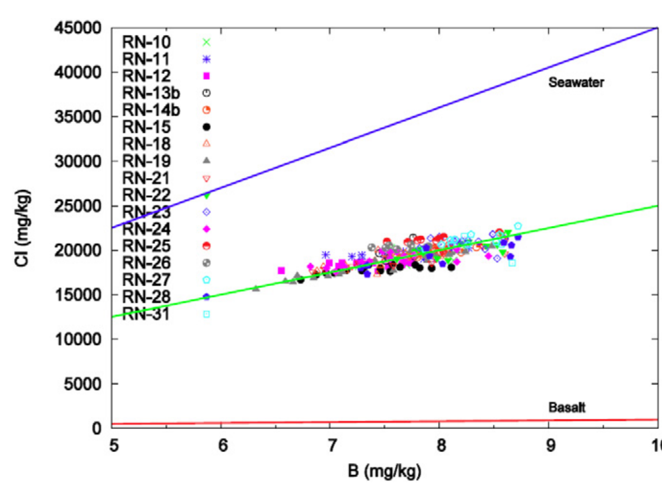

Fig. 7. Chloride concentrations against boron concentrations in the Reykjanes deep liquid. The lines represent extrapolations of the Cl/B ratios in seawater (blue), Icelandic basalt (red) and the average for the Reykjanes liquid (green). From Óskarsson and Gałeczka (2017).

The Cl/B ratio in the Reykjanes fluids is very homogeneous and lies between the ratios for seawater and basalt. This may be due either to rock dissolution or to the addition of a B-rich magmatic gas. Thermodynamic calculations indicate that the concentrations of the reactive gases H_2S and H_2 are controlled by temperature dependent equilibria with minerals; possibly anhydrite, wollastonite, magnetite, quartz, and pyrite. N_2 and Ar, on the other hand, appear to be controlled by the solubility of these gases in water (Óskarsson and Gałeczka, 2017). At the onset of production, excess N_2 and He, possibly of magmatic origin, appear to have accumulated in the reservoir, but samples collected in 2013 showed that the concentrations of these gases had decreased drastically since 2007 (Óskarsson et al., 2015b).

The only observation that contradicts the seawater origin theory is low ratio of deuterium in the hydrothermal fluids. The oxygen isotopes in the fluid vary from ~−1 to 2‰ with an average value near seawater (Pope et al., 2009). In contrast, geothermal solutions at Reykjanes have δD ranging from −15 to −25‰ (relative to SMOW), whereas seawater has δD ≈ 0‰, as do most seafloor hydrothermal fluids (Shanks, 2001). Pope et al. (2009) suggested that the low deuterium values could be explained by isotope exchange between seawater and hydrous secondary minerals (epidote, chlorite, smectite) formed under pre-Holocene conditions when the geothermal fluids at Reykjanes were likely of meteoric origin, in a system that was probably fed by glacial melt-water. This hypothesis is supported by studies on fluid inclusions in drill cuttings from Reykjanes which have suggested that a low- to high-salinity transition has taken place in the reservoir since the last glaciation (Franzson et al., 2002). However, in their modeling Pope et al. (2009) assumed that the Reykjanes reservoir is a closed system and that the residence time of water must be very long in order that isotope equilibrium to be reached. With elevated fluid recharge rates due to production, the fluids should have a shorter time to reach isotopic equilibrium and therefore would be predicted to become less depleted in deuterium with time. This has not been observed during the first 10 years of production (Óskarsson and Gałeczka, 2017), in which fluid is estimated to have been extracted from about 1.2 km^3 of rock (Axelsson et al., 2015).

Geochemical monitoring in Reykjanes has been ongoing since the first discharge of well RN-8 in 1970, but little changes were noticed before the commissioning of the 100 MWe power plant in 2006. Since 2006, the geochemical monitoring has been more frequent, and some changes in the reservoir fluid composition have been observed. In the first years of production an increase was observed in the concentrations of most solutes, including Cl (Fig. 6). These changes were most prominent in wells producing from the SW part of the production field and were taken to be caused by progressive boiling of the reservoir fluid in response to the production-induced pressure decline in the reservoir. This trend levelled off in 2011–2012 and has since been masked by a decrease in solute concentrations in most parts of the field (Fig. 6), particularly the NE part. Reservoir tracer tests have confirmed that this latter trend is caused by the re-injection of a less saline mixture of separated brine and condensate. This development is discussed in greater detail by Óskarsson et al. (2015a).

6. Initial results of the IDDP-2 well

Siting the IDDP-2 well took advantage of the extensive knowledge already gained during the exploration and development of the field for power production. It was evident that the main upwelling zone for the hydrothermal system lies between wells RN-15 and RN-17 and that deep permeability is controlled by a fracture system along the axis of the rift (Fig. 3). The field operator, HS Orka, made a 2.5 Km deep vertical production well, RN-15, available to the IDDP for deepening (Fig. 3). The details of drilling the RN-15/IDDP-2 have been described by Stefánsson et al., 2017 and Friðleifsson et al., 2017. Drilling began by deepening the RN-15 from 2.5 km to 3 km and casing it with 9 7/8″–9 5/8″ casing, cemented to the surface. To reach the main upflow zone and intersect vertical fractures at depth, the deeper part of the well was directed along an azimuth of 210°, with a kick off point at a depth 2750 m, inclined from the vertical at 16°, but increased considerably near the end of drilling and approached ~36° at the bottom. The surface projection of the bottom of the well is 738 m SW of the wellhead of RN-15, with a vertical depth of about 4.5 km. Drilling, casing, cementing, and spot coring took 168 days.

Various challenges arose as the drilling progressed; there were weather delays, problems with hole stability that required frequent reaming, and the drilling assembly becoming stuck several times. Each of these issues was solved successfully. However, as mentioned earlier, the major problem that was not solved was a complete loss of circulation returns to the surface encountered at depths just below the production casing shoe. The circulation loss could not be cured with lost circulation materials, nor by 12 successive attempts to seal the loss zone with cement. Therefore, drilling had to continue with only intermittent cutting returns between 3000 and 3180 m depth and no return of drill cuttings from deeper than 3180 m. It appears that an amount of rock equal to the total volume of the drilled well (~60 m^3) disappeared as drill cuttings into this loss zone. Consequently, the limited number of spot drill cores that the science budget allowed were the only deep rock samples recovered from the IDDP-2.

Because it is nearly twice as deep as any previous well in the Reykjanes field, the IDDP-2 has provided the only direct measurements of temperatures and fluid pressures deeper than 2.7 km in the reservoir. The first pressure-temperature logs to indicate the well had reached supercritical conditions were obtained on January 3rd, 2017, after allowing the well to heat for only 6 days after circulation of drilling fluid (Weisenberger et al., 2017). At that time, a 7″ liner had just been inserted into the well to facilitate injection of cold water to enhance permeability deep in the well by thermal fracturing. Fig. 8A shows the temperature-pressure (T-P) log from that logging run. It indicates that at 4560 m depth, close to the bottom of the well, the measured temperature is 426 °C at a fluid pressure of 34.0 MPa. The inflection point in the temperature log at ~3400 km, is due to cooling at the major circulation loss zone. There are also deeper and smaller loss zones at ~4375 m and at ~4500 m slant depths.

As we have not yet sampled the deep formation fluids in the IDDP-2, we do not know their composition. It is presumably modified seawater from the recharge that is diluted with drilling fluid (fresh water with minor additives). Whatever the fluid composition at 4.5 km depth, it is hard to argue that the measured temperatures and pressures are not supercritical. However, one caveat is that the measurements were acquired by a K-10 logging tool that was calibrated only to 380 °C.

It is clear from the temperature profile shown in Fig. 8A, that these measurements were made when the well was far from thermal equilibrium. At that time, 40 L/s cold surface water was being injected to cool and control the well. We could therefore expect that when thermal recovery is complete the maximum temperature would certainly exceed 426 °C.

In late May 2017, a second week-long heating-up experiment was carried out. Four successive temperature logs were measured, this time using a Kuster bimetal logging tool calibrated over the range from 120 °C to 440 °C (Fig. 8B). During these measurements approximately 5 L/s of cold water was being injected down the annulus between the well and the 7″ stimulation liner string.

The data for the 26th and 29th of May show considerable cooling at the 4500 m loss zone, indicating that the cold-water injection or "soft" stimulation has been successful in increasing permeability in this supercritical zone.

The purple stars in Fig. 8B show calculated equilibrium formation temperatures (FT), using the Horner method (Horner, 1951), at several logging points on the warm-up T-logs. The highest temperature estimate is 535 °C at approximately 4615 m slant depth. For comparison, Fig. 8B also shows the boiling point versus depth curve (BPD) for seawater assuming a water table at 450 m depth

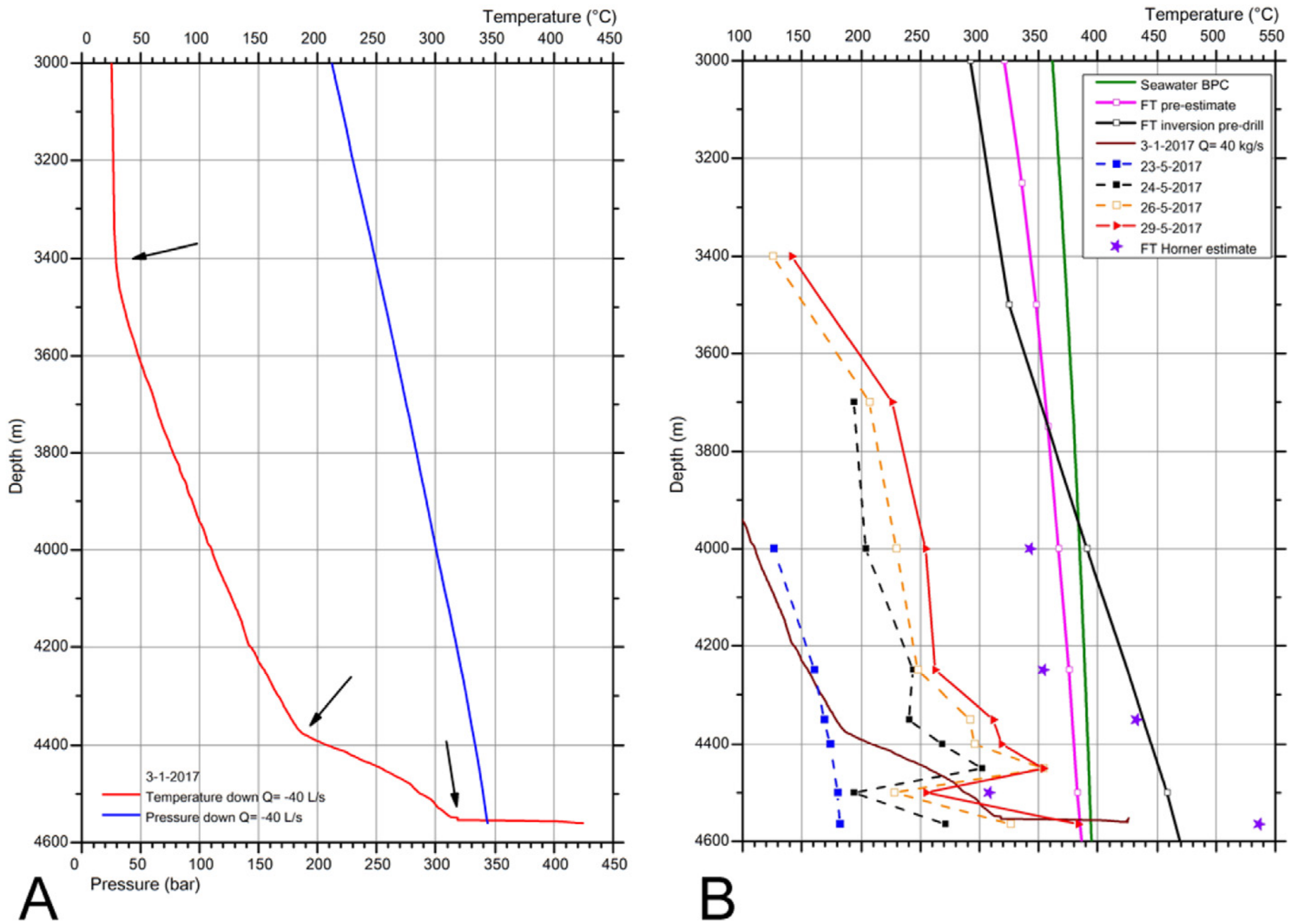

Fig. 8. A and B. The T-P log (A) shows the temperature T (red line) reaching 426 °C and pressure P (blue line) reaching 34.0 MPa at the bottom of the well. Three feed zones, present at ~3400 m, ~4375 m and at ~4500 m, are indicated by blue arrows. A compilation of several temperature profiles (B), including the one shown in (A), beginning at 100 °C and 3950 m depth. Other T logs shown were measured on the 23d, 24th, 26th, and 29th May 2017, in a weeklong heat-up interval during the stimulation program. The three T profiles shown by black, violet and green solid lines represent estimated formation temperatures based on geophysical inversion (Hokstad and Tänavsuu-Milkeviciene, 2017), a pre-drilling temperature estimate based on an extrapolated T-gradient in RN-15 (Friðriksson et al., 2015, and a boiling point with depth (BPD) curve for seawater (calculated for a water-table present at 450 m)). Finally, purple stars indicate formation temperatures based on Horner plot estimates from the warm-up T logs. The purple star near the bottom of the diagram gives a temperature value of ~535 °C.

(green line), and a temperature gradient extrapolated from measurements of RN-15 (pink line) prior to deepening (Friðriksson et al., 2015). Hokstad and Tänavsuu-Milkeviciene (2017) have also estimated the formation temperature by a Bayesian inversion of multigeophysical data.

Their FT-inversion pre-drilling estimate is represented in Fig. 8B by the black line that ends at 470 °C at 4600 m depth. Hokstad then used logging data collected during drilling of the RN-15/IDDP-2 well, for a new joint inversion that suggests still higher formation temperatures of 535 °C (±50 °C) at 4500 m (Fig. 9), similar to the temperature estimated using the Horner method at that depth.

Since drilling the IDDP-2 ended, the well has been controlled and permeability stimulation attempted by injecting cold fresh water at a rates of 5–10 L/s. However, late in 2017 a problem within the production casing was detected. Deploying logging tools is now prevented by a constriction in the 9 5/8″ production casing between 2307 and 2380 m depth. As repair of this constriction would be difficult and expensive, the current consensus is to carry out flow testing without a repair of the casing. Cold water injection was continued until early August 2018 when injection of hot water began. This will be followed by a gradual warm-up period in preparation for long-term flow tests in early 2019. This should allow sampling of the deep supercritical formation fluids, and more tightly constrain the actual formation temperatures.

7. Seismic activity during the IDDP-2 drilling

Seismic activity in Reykjanes is variable over time, with scattered activity and occasional short-term earthquake swarms. Since the beginning of 2013, a dense local seismic network of seven seismic stations with an average spacing of ~0.5 km has been in operation around the Reykjanes geothermal field. In addition, on-line data from four seismic stations in the regional seismic network of Iceland (the SIL network) are available. Seismic activity was closely monitored during the IDDP-2 drilling from the 12th of August 2016 to the 25th of January 2017. During this period 650 earthquakes occurred in the Reykjanes area and more than 200 of them were located within <1 km of the RN-15/IDDP-2 wellhead (Fig. 10).

Scattered earthquake activity was ongoing during drilling, with a maximum daily rate of 12 earthquakes occurring on the 15th of October 2016. Comparison of hypocentral depths with daily reports on the drilling progress, starting at 3 km depth, indicates that induced earthquakes seem to follow the drill bit with time. Earthquake activity mainly occurred within the depth range where drilling activity took place, i.e. 3–5 km (Fig. 11).

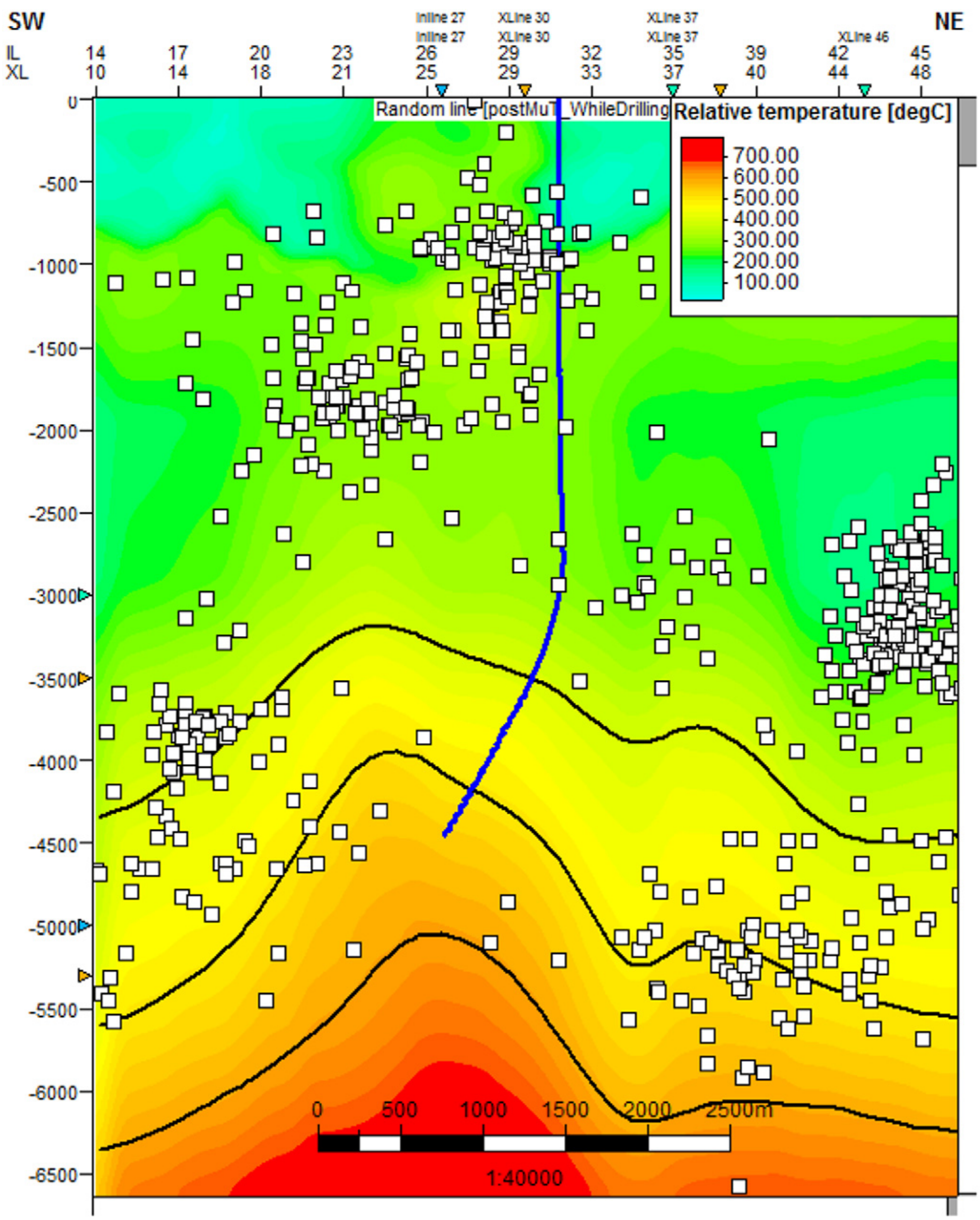

Fig. 9. Temperature prediction based on multi-geophysical inversion and data collected during drilling (from Hokstad and Tänavsuu-Milkeviciene, 2017). Black lines indicate 400 °C, 500 °C and 600 °C isotherms with increasing depth. The blue line is the actual path of the IDDP-2 well. White squares indicate the focal points of earthquakes detected by the seismic array at Reykjanes prior to drilling. Earthquakes are sparse at temperatures above ~550 °C, and few were detected below ~3 in the fluid up flow zone prior to drilling.

The brittle-ductile boundary at Reykjanes is generally believed to occur at 5.5–6 km depth (Guðnason et al., 2015), but earlier observations from the local seismic network also revealed an aseismic body between 3 and 6 km depth beneath the center of the production field of Reykjanes (Fig. 9). The apparent size of this aseismic body was reduced somewhat by including older data from the national network. However, the uppermost part of this inferred aseismic body, from 3 to 5 km depth, became seismically active during the deep drilling (Guðnason et al., 2016). A possible explanation for the absence of natural earthquakes in this body is that its temperature is very close to the brittle-ductile boundary for normal strain rates. Presumably, the introduction of cold water into the zone of total circulation below 3.0 km depth increased the strain rate sufficiently to induce seismicity. This opens the possibilities to put better constraints on the temperature of the brittle-ductile boundary of basaltic crust in general. This group of induced earthquakes follows a trend striking NW-SE. These earthquakes are predominantly small, with magnitudes ranging from 0.5 to 1.9 M_L, with 95% of located earthquakes ranging from 0.5 to 1.5 M_L.

8. IDDP drill cores at Reykjanes

Studies of drill cuttings recovered from Reykjanes geothermal wells have provided important insights into the complexities of fluid evolution and temperature fluctuations in the production zone of the Reykjanes system (Franzson et al., 2002; Friðleifsson et al., 2003, 2005; Marks et al., 2010, 2011, 2015). However, drill cuttings are not ideal samples because recovery is biased towards more resistant alteration minerals, mixing occurs over significant depth intervals, and drill cuttings from greater depths are commonly of smaller grain size than those from shallower levels, (Fowler and Zierenberg, 2016a). Although taking drill cores while drilling a production well is expensive in terms of rig time, study of drill cores is highly preferable to studying

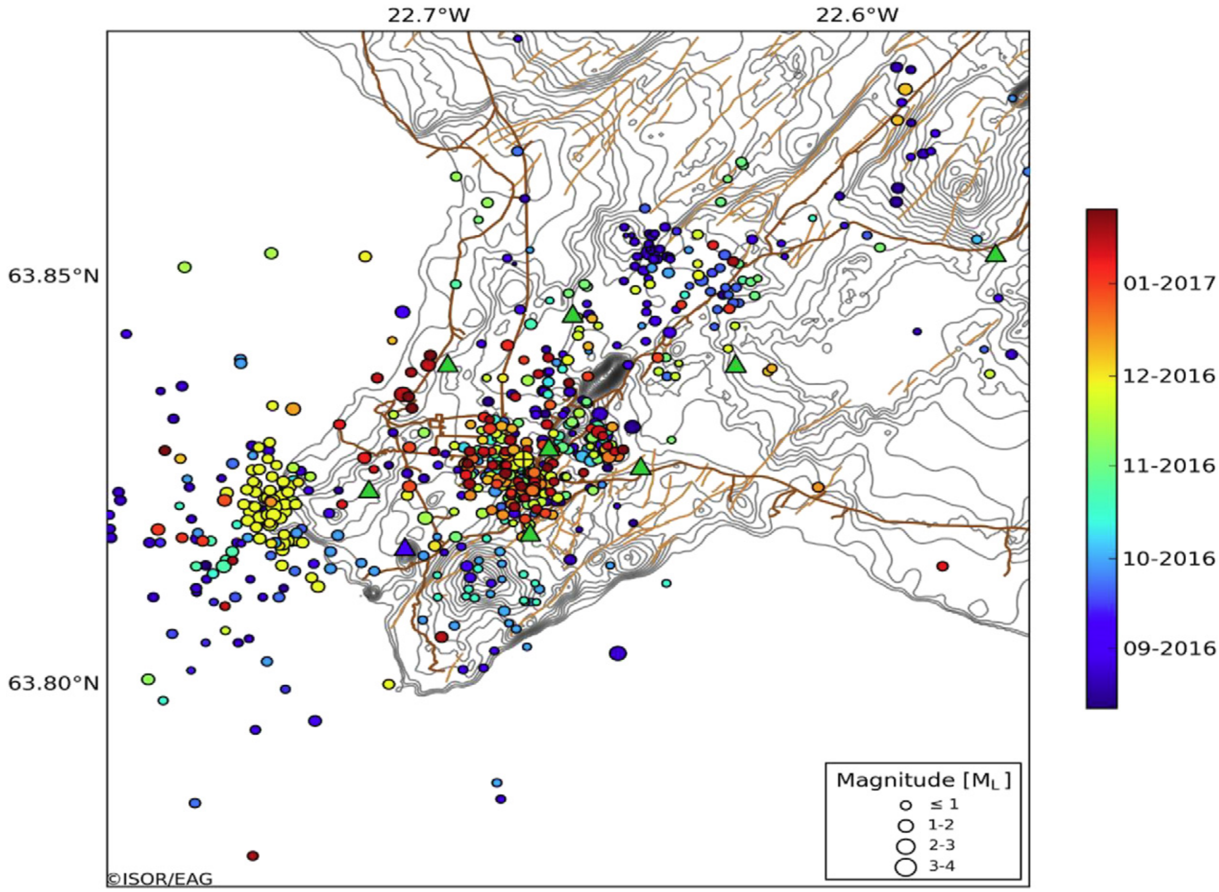

Fig. 10. Location of earthquakes in Reykjanes during the IDDP-2 drilling, colored according to time of occurrence and sized according to magnitude. The IDDP-2 wellhead is shown with a yellow cross, seismic stations with green triangles and a SIL seismic station with a blue triangle. The cloud of earthquakes near the SW corner of the peninsula represents a tectonic event late November.

drill cuttings from deep levels in a geothermal system, especially when petrological and petrophysical data are important.

There were no drill cores available from the Reykjanes field until the IDDP began operations there. In preparation for deep drilling, cores were taken from the upper 3 km of the field, firstly to test a custom-made 10 m-long IDDP coring assembly, designed with extra cooling, and custom-made PCD drill bits designed to operate at high-temperatures, and, secondly, to learn more about the petrology and petrophysics of the upper 3 km of the field that would not be sampled while drilling the IDDP-2. Fig. 12 shows the location of wells from which the IDDP obtained drill cores, RN-17B, RN-19, RN-30 and IDDP-2.

RN-19 is a vertical well located on the edge of the main geothermal production area (Fig. 12). A 2.7 m long core was drilled in April 2005

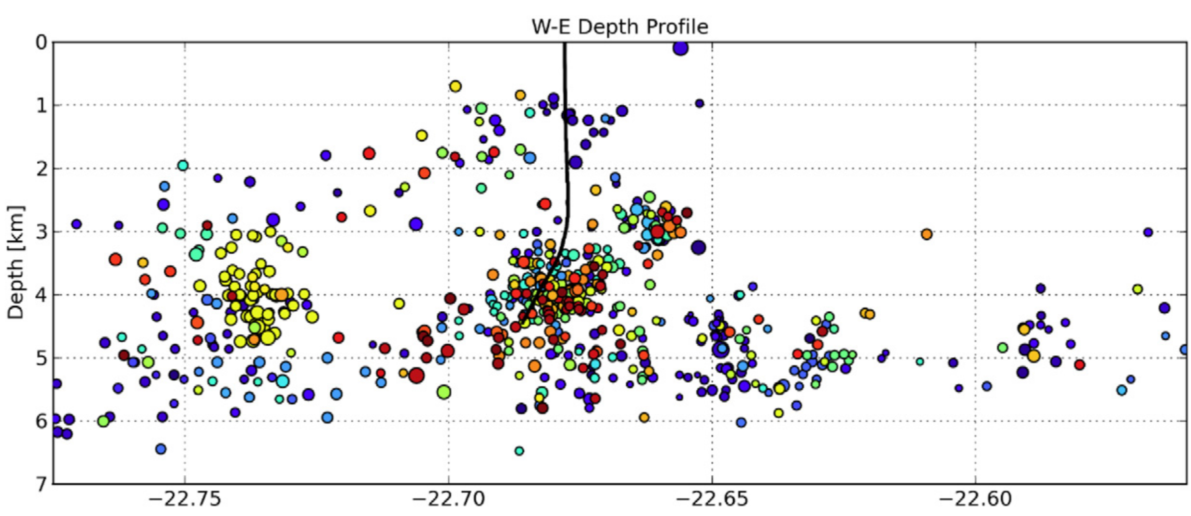

Fig. 11. W-E depth profile of earthquakes located in Reykjanes during the IDDP-2 drilling, colored according to time of occurrence and sized according to magnitude. The coloring is the same as that in Fig. 10. The trajectory of the IDDP-2 well is shown with a black line.

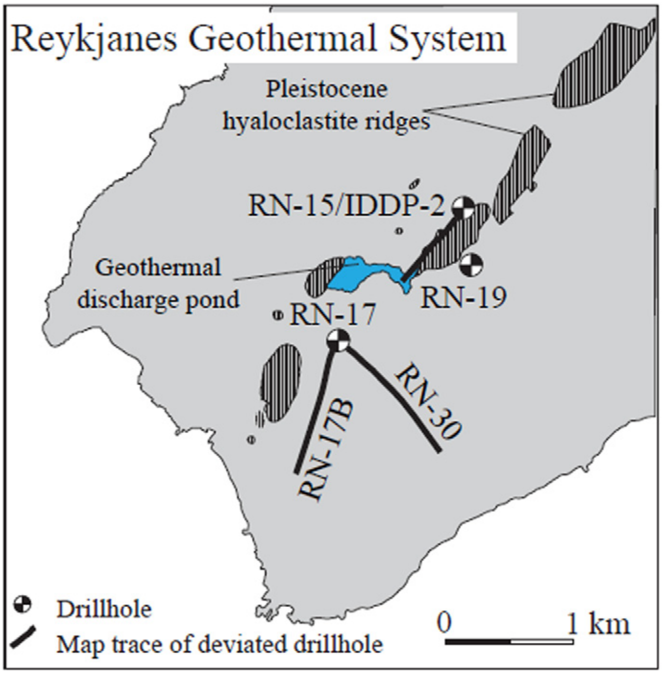

Fig. 12. Map showing the location of drill holes in the Reykjanes geothermal field where spot cores have been obtained by IDDP, i.e. RN-17B, RN-19, RN-30 and RN-15/IDDP-2.

from a depth of 2245 m at an in-situ temperature of 275 °C. The core is composed of coarse crystalline dolerite coming from a sheeted dike complex (Friðleifsson et al., 2005; Mortensen et al., 2006; Friðleifsson and Richter, 2010). The RN-19 core is the coarsest-grained and least altered sample of basaltic intrusive rock recovered from Reykjanes to date, with plagioclase and clinopyroxene phenocrysts in the size range 2–3 mm (Fig. 13C). Fowler and Zierenberg (2016a) showed that the RN-19 core belongs to the trace element depleted basalt category of Gee et al. (1998), a rock type typically associated with picritic basalts that are found in <2% of surface exposures on the Reykjanes Peninsula (Jakobsson et al., 1978).

RN-17B is an inclined hole side tracked to the south southwest from the RN-17 well pad, with an inclination of about 35° from vertical starting at depth of 933 m (Fig. 12). A 9.3 m core was drilled in RN-17B in November 2008, at a starting downhole depth of 2798.5 m (true vertical depth ~2560 m) and an in-situ temperature of 345 °C. The core is composed of a series of basalt pillows, hyaloclastite, lithic breccia (examples in Fig. 13A and B), and volcanic sandstone units (Friðleifsson et al., 2005; Friðleifsson and Richter, 2010; Fowler et al., 2015; Helgadóttir et al., 2009). The rocks recovered from RN-17B share many characteristics of axial volcanic ridge deposits observed offshore along the submarine Reykjanes Ridge (Fowler et al., 2015). The presence of shell fragments replaced by epidote indicates some of the RN-17B sedimentary material was derived from relatively shallow water. This suggests that this formation has experienced a high rate of subsidence (Friðleifsson and Richter, 2010). The concentration of relatively immobile trace elements indicates that these rocks are related to the trace element enriched category of Gee et al. (1998), similar to the tholeiitic lava flows that cover most of the Reykjanes peninsula. The pattern of alteration-induced gains and losses of elements recorded

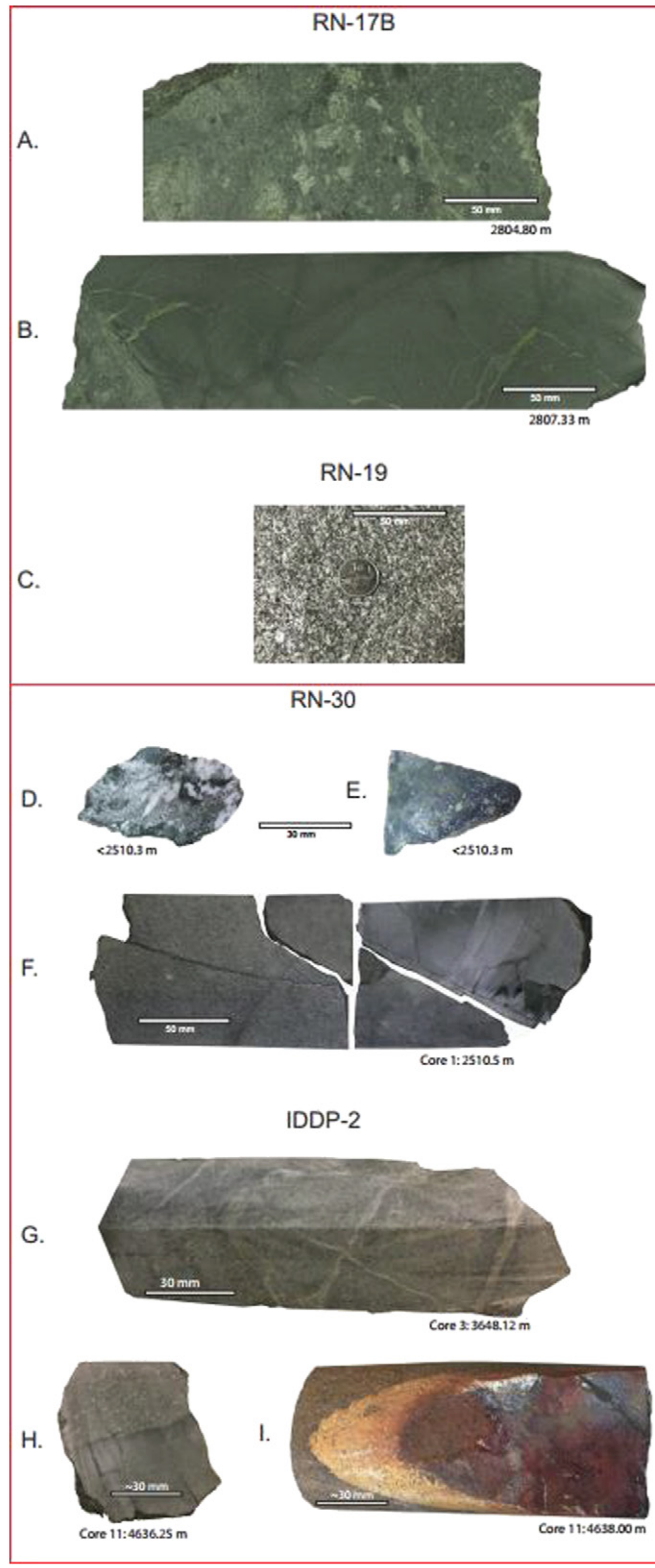

Fig. 13. A, B, C. Examples of drill core recovered by IDDP drilling efforts. (A) heterogenous lithic breccia from the RN-17B core interpreted to have formed on an axial volcanic ridge. (B) Basalt pillow/basalt flow lobe with a quenched margin and prominent epidote veins from the RN-17B core. (C) Coarse crystalline dolerite recovered in the RN-19 core. D, E, F, G, H, I. Examples of drill core recovered by IDDP drilling. (D) Highly altered silicified hyaloclastite cut by quartz-epidote-anhydrite veins, from a slough block from above the RN-30 drill core. (E) Glassy vesicular basalt pillow margin or flow lobe edge replaced by quartz and epidote, from a slough block above the RN-30 drill core. (F) Two dolerite half dikes separated by a chilled margin near the top of the RN-30 core. (G) Highly altered dolerite from core 3 in the IDDP-2 well. (H) Two dolerite half dikes separated by a chilled margin from core 11 in the IDDP-2 well. (I) Quartz-plagioclase rich plagiogranite segregation vein in dolerite from core 11 in the IDDP-2 well. Red stains are hematite, formed as cold oxidizing drilling fluids contacted hot reducing ferrous-rich hydrothermal fluids.

in the RN-17B core, relative to an unaltered precursor, suggests emplacement on the seafloor and passive alteration by seawater, followed by subsidence, burial, and alteration at progressively higher temperature conditions (Fowler and Zierenberg, 2016b).

RN-30 is also inclined at depth at an angle of ~35° heading southeast and was drilled from the same well pad as well RN-17 (Sigurgeirsson et al., 2011). A total of 22.5 m of core was drilled from three sequential intervals in May 2011, from a starting downhole depth of 2510 m (true vertical depth ~2250 m) and an in-situ temperature of 345 °C. The cores are composed of a series of fine- to coarse-grained dolerite intrusions of basaltic composition (example in Fig. 13F), interpreted to come from a sheeted dike complex (Fowler and Zierenberg, 2016b). The location of RN-30 rocks immediately below the Skálafell shield volcano suggests at least some of the intrusions may be feeder dikes for that edifice, but confirmation studies are needed. It is interesting that at least two of the dikes recovered in RN-30 fall into Gee et al. (1998) trace element depleted suite. They share trace-element distribution patterns with olivine-tholeiite/picritic lavas such as those erupted at the Háleyjabunga lava shield (see Fig. 3) east of the Reykjanes geothermal field. Rocks from stratigraphically higher intervals in the RN-30 hole were recovered as slough blocks on top of the RN-30 cores (Fig. 13D and E), that were originally vesicular glassy basalt, hyaloclastite, and volcanic siltstone, but these rocks are extremely altered with extensive leaching and silicification. The rocks are cut by quartz, epidote, and anhydrite veins (Fowler and Zierenberg, 2016b) and may be an example of recharge-related alteration in a major geothermal aquifer. While the chemistry of the RN-30 cores is compatible with a single-stage of alteration at the in-situ conditions, the slough blocks have undergone a complex prograde alteration history, like that in RN-17B rocks (Fowler and Zierenberg, 2016b).

9. Hydrothermal alteration

A series of indicator minerals and rock textures that occur at progressively higher temperatures have been recognized previously in Icelandic geothermal systems, in part facilitated by IDDP drilling (Tomasson and Kristmannsdottir, 1972; Schiffman and Friðleifsson, 1991; Lonker et al., 1993; Marks et al., 2010). Successive alteration minerals that appear with increasing temperatures in the Reykjanes system include: mixed-layer smectite–chlorite, chlorite, mixed layer chlorite–illite, epidote-actinolite, amphibole, and pyroxene (Marks et al., 2010; Zierenberg et al., 2017). At the most extreme conditions, interpreted to be related to diking events, drill cuttings are recrystallized with granoblastic textures and secondary clinopyroxene and ortho pyroxene formed at temperatures in excess of 925 °C (Marks et al., 2011; Schiffman et al., 2014).

Of the IDDP cores, dolerite in the RN-19 core is the least altered rock with fresh igneous clinopyroxene, plagioclase, and magnetite (Fig. 14A and B). Localized alteration is confined to replacement of late-stage interstitial melt and clinopyroxene rims chlorite/actinolite which also occurs as rare thin, discontinuous veins (Fowler and Zierenberg, 2016b).

Alteration of RN-30 dolerite is more extensive than that in RN-19, although the extent varies depending on the relative age of each dike. Generally, the material interstitial to major igneous minerals is completely altered to chlorite (±albite, actinolite, quartz, apatite, chalcopyrite), clinopyroxene edges are incipiently replaced by actinolite/hornblende, and there is incipient replacement of igneous plagioclase with albite (Fig. 14C and D; Fowler and Zierenberg, 2016b).

In the oldest RN-30 dikes (age based on chilled dike margin relationships), there are sparse epidote + quartz in vugs and the core is cut by wispy epidote veins.

Rocks in the RN-17B core are variably altered to greenschist and amphibolite facies mineral assemblages (Fowler et al., 2015). Prominent epidote ± pyrite veins with actinolite and chlorite selvedges are common in RN-17B. Temperature/salinity relationships of fluid inclusions suggest portions of epidote veins formed from modern geothermal conditions, while others suggest a temperature spike in the past possibly related to adjacent intrusion of a dike. The interiors of crystalline clasts and basalt pillows are largely replaced with chlorite, and incipient amphibole is actinolitic in composition relative to more pervasive hornblendic amphibole in glassy clast exteriors and replacing glassy hyaloclastite fragments (Fig. 14E and F). Plagioclase laths retain their igneous texture, but many have calcic (up to An_{99}) compositions, and coupled with hornblendic amphibole compositions, indicating incipient amphibolite grade alteration. The disequilibrium assemblage of greenschist and amphibole grade indicator minerals suggest the RN-17B rocks may be actively transitioning to an amphibole grade assemblage at the in situ 345 °C owing to subsidence to higher P-T conditions. The bulk rock composition, secondary mineralization, and fluid inclusion petrography of RN-17B rocks suggest a complex history of fluctuating P-T conditions and fluid composition (Fowler et al., 2015; Fowler and Zierenberg, 2016a). Alternatively, the disequilibrium secondary mineral assemblage may reflect periodic spikes in the local temperature environment in response to adjacent diking events that promotes the formation of amphibolite grade minerals.

10. IDDP-2 drill cores

Because of the total loss of circulation in the IDDP-2 well below 3200 m depth, the spot cores are the only rock samples available from deeper than 3.1 km (Table 1). Coring proved difficult in these conditions with the equipment available, and although thirteen coring attempts were made, coring in total 43.3 m, only 27.3 m of cores were recovered.

The IDDP-2 cores include a series of dolerite dikes with chilled margins (Fig. 13G & 13H) interpreted to come from a sheeted dike complex (Zierenberg et al., 2017). Many of the rocks that sloughed onto the cores from unknown depths above drilling intervals include dolerites, basalts, and a few hyaloclastite and volcanic sandstone/siltstones with alteration similar to the RN 17B and RN 30 cores. The core samples recovered from IDDP-2 differ from those in the other Reykjanes wells in the alteration style and extent of alteration (see below), and uniquely include felsic segregation patches of the last melt fraction that form thin plagiogranite veins/dikes in core 10 and below (Fig. 13 I). IDDP-2 drill cores 10–13 recovered the first examples of felsic intrusive rocks on the Reykjanes peninsula; southwest of Hengill, a major volcanic complex to the north (Fig. 1).

Although many of the core samples show pervasive alteration, cross cutting veins are relatively uncommon and open space filling veins are nearly absent. Alteration assemblages show that the rocks have not completely attained an equilibrium mineral assemblage reflective of the current P-T conditions. These rocks record a complex history of response to adjacent dike emplacement and variable hydrothermal conditions. Further study promises to reveal insights into the longevity and transient conditions near the roots of hydrothermal circulation.

Dolerite alteration and vein mineralogy in the shallowest IDDP-2 cores (i.e. core 3; Fig. 14G & H) bears many similarities to that in the RN-17B core. The shallowest IDDP-2 rocks are extensively veined by epidote, amphibole, plagioclase ± quartz with chlorite-rich vein selvages (Fig. 13 G). Igneous clinopyroxene is completely replaced with actinolite/hornblende ± chlorite, and plagioclase has secondary calcic domains and appears dusty with abundant secondary mineral and fluid inclusions (Fig. 14G and H). The presence of hornblende and calcic plagioclase is an indication that the rocks have reached P-T conditions of the amphibole alteration facies, but the rocks have not reached equilibrium, possibly reflecting prograde expansion of the hydrothermal system and/or subsidence of these rock to higher T, P conditions (Zierenberg et al., 2017). Fluid inclusion and alteration mineral paragenetic studies are ongoing to determine the range of P-T conditions and fluid compositions that IDDP-2 rocks have experienced.

In contrast to shallower IDDP cores, chlorite and epidote are absent from core 5 and below (i.e. below ~ 3865 m), thus, amphibolite grade P-T conditions prevail. In most of the cores, igneous clinopyroxene is

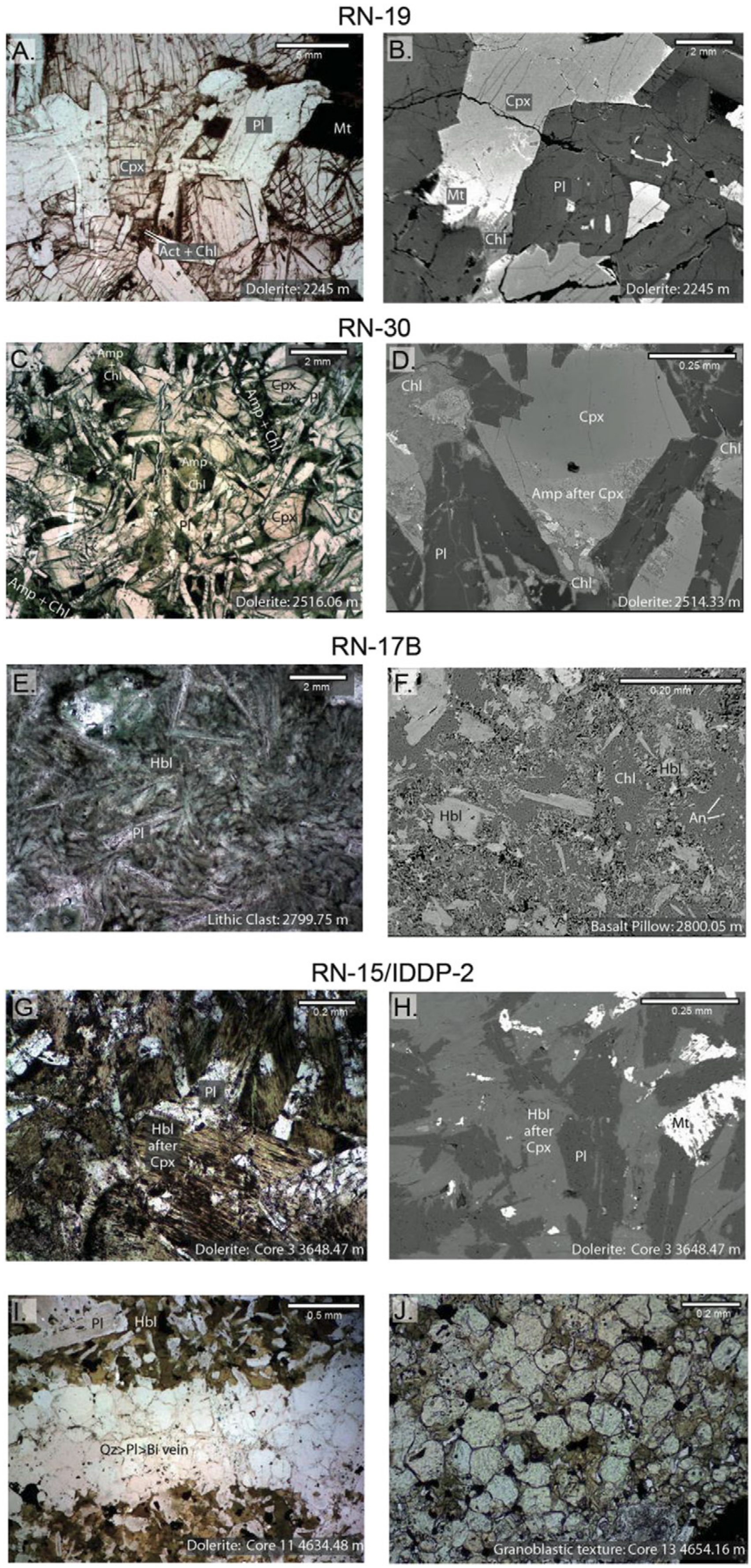

Fig. 14. Plane polarized light (ppl) and back scattered electron (BSE) images of secondary alteration in IDDP core samples. See text for descriptions.

Table 1
Summary of drill core recovered from the IDDP-2 well.

Core run	Coring interval	Cored length [m]	Core recovered [m]
1	3068.7–3074.1	5.4	0
2	3177.6–3179.0	1.4	0
3	3648.0–3648.9	0.9	0.52
4	3648.9–3650.7	1.8	0
5	3865.5–3869.8	4.3	3.85
6	3869.8–3870.2	0.4	0.15
7	4089.5–4090.6	1.1	0.13
8	4254.6–4255.3	0.7	0.28
9	4308.7–4309.9	1.2	0
10	4309.9–4311.2	1.3	0.22
11	4634.2–4642.8	8.6	7.58
12	4642.8–4652.0	9.2	9
13	4652.0–4659.0	7	5.58
Total		43.3	27.31

pervasively to completely altered to amphibole. Actinolite persists at depth, but hornblende becomes increasingly abundant downhole. At the bottom of the hole (Core 11–13), hornblende alteration is accompanied by secondary clinopyroxene and orthopyroxene. Plagioclase retains its original igneous textures and nominally appears to be little altered. Albitization of plagioclase is minor to absent in the deeper cores, but the plagioclase is often cloudy due to an abundance of vapor-rich fluid inclusions and the compositions show a wide range from andesine to anorthite. The dominant vein minerals are amphibole and calcic plagioclase, which can occur separately or together. Plagioclase rich veins may contain minor amounts of quartz, but quartz is absent from most hydrothermal veins cutting dolerite, but is locally abundant in replacement veins in and adjacent to the plagiogranite segregation patches and veins (Fig. 14I). Although most of the cores show pervasive alteration, cross-cutting veins are volumetrically a very minor component of the rock. The veins tend to be thin (1–4 mm), irregular and discontinuous and lack evidence filling of open space, consistent with formation in the brittle/ductile transition zone. Trace amounts of hydrothermal biotite is noted as shallow as Core 8 (4254 m) and become more abundant at depth.

The most continuous core recovery was achieved at the bottom of the hole from 4634 to 4659 m. Most of the dikes in this section show pervasive alteration of igneous clinopyroxene to hornblende, which is locally intergrown with secondary clinopyroxene and orthopyroxene. Hydrothermal biotite is less abundant than amphibole, but it is intergrown with hornblende and secondary pyroxene in the deeper rocks.

There is patchy development of recrystallized granoblastic textured clinopyroxene, which is locally intergrown with hydrothermal orthopyroxene ± hornblende (Fig. 14J). These patches record hydrothermal alteration at the transition from magmatic to hydrothermal conditions. Plagio-granite segregation veins are more common in the deepest cores. The shallower veins are dominantly intermediate plagioclase and quartz with minor clinopyroxene, most of which has been altered to hornblende. The deepest felsic veins also have minor amounts of igneous biotite, which has higher F and Cl content compared to hydrothermal biotite developed in dolerite. Apatite is a relatively abundant trace mineral in the felsic veins and some veins have sparse euhedral zircon.

The alteration of the deeper Reykjanes rocks is remarkably like that of hydrothermally altered oceanic crust (Fig. 15; Marks et al., 2010; Fowler et al., 2015; Fowler and Zierenberg, 2016b; Zierenberg et al., 2017). The IDDP core samples thus provide a unique opportunity to investigate water-rock reaction processes actively occurring in the roots of such submarine 'black smoker' hydrothermal systems. This has not previously been possible because the drill cores obtained by ocean drilling were recovered from older crust that can be overprinted with generations of subsequent low temperature alteration as oceanic crust migrated away from the spreading center.

Although drilling the IDDP-2 was significantly more expensive and technically challenging than drilling a conventional geothermal production well, it was significantly less so than drilling an active mid-ocean ridge at sea from a dynamically positioned drill ship.

11. Petrophysical properties of IDDP core samples from the Reykjanes geothermal field

Reliable data on the physical properties of rocks is of major interest for a realistic interpretation of geophysical and wireline log measurements necessary for predicting reservoir potential. This is particularly the case when considering supercritical reservoirs, whose conditions of pressure and temperature are difficult to replicate at the laboratory scale. Up to now, laboratory petrophysical investigations at high temperature and pressure have been restricted largely to dry conditions and did not account for the effect of a pore fluid pressure on the physical properties of rocks. For technical reasons, experimental set-ups with flow of pore fluid flow have been restricted to <250 °C (e.g. Kristinsdóttir et al., 2010). Recent technical developments have allowed measurement of some physical properties, such as electrical conductivity and permeability, under pore fluid pressure, confining pressure and temperature that are expected deep in geothermal reservoirs, under supercritical conditions (e.g. Kummerow and Raab, 2015; Nono et al., 2017) and up to magmatic conditions. We are now able to investigate the physical behavior of samples under in-situ conditions at the laboratory scale, including samples from all of the Reykjanes drill cores. Intensive geophysical surveys of this area offer an excellent opportunity to compare small scale investigations to large scale geophysics, leading to a better understanding of geophysical signals in terms of rocks properties and in-situ conditions.

Several core samples from wells RN-17B, RN-19, RN-30 and IDDP-2 were made available for petrophysical investigations at the Laboratoire Geosciences Montpellier (Table 2). They were mostly dolerites, except for one hyaloclastite (RN-17B), and all display high temperature alteration. Mineralogy was determined by XRD and SEM analysis. Conventional petrophysical characterization at ambient conditions was performed on several mini-cores (25.4 mm in diameter) subsampled from the larger drill cores. To characterize the pore space topology, triple weight, mercury and helium porosities, and sonic velocities, permeability, and electrical parameters, such as formation factor and surface conductivity, were determined. Dolerites display a low porosity, mostly resulting from inter- or intra-granular fractures, while hyaloclastites display a high porosity and behave macroscopically as a granular medium. The high level of micro-fracturing in dolerites may have been induced during drilling operations, i.e. rapid mineral contraction during cooling, and is mostly observed on samples from IDDP-2. A subset of the mini-cores was selected for measurements at high-temperature and high-pressure in a gas pressure apparatus (Paterson Press) at Geosciences Montpellier. Major results are summarized in Table 2 (From Escobedo et al., 2017; Nono et al., 2016a,b; and Nono et al., 2017).

To investigate the effect of pressure and temperature on the pore network, permeability was measured with argon as a pore fluid, to avoid fluid-rock interactions. Pore pressure was fixed at 20 MPa, while confining pressure and temperature were varied from room conditions to 150 MPa and 800 °C, respectively. Measurements indicate that the permeabilities of dolerite strongly decreases with increasing confining pressure and reach very low values at reservoir conditions (10^{-19}–10^{-20} m^2 s^{-1}), as expected for micro-cracked crystalline rocks where micro-cracks close with pressure, while it remains nearly constant for the hyaloclastites where the permeability is about 10^{-16}–10^{-15} m^2 s^{-1}. Increasing temperature does not modify the permeability significantly, except for the RN-19 sample where an irreversible increase by two orders of magnitude is

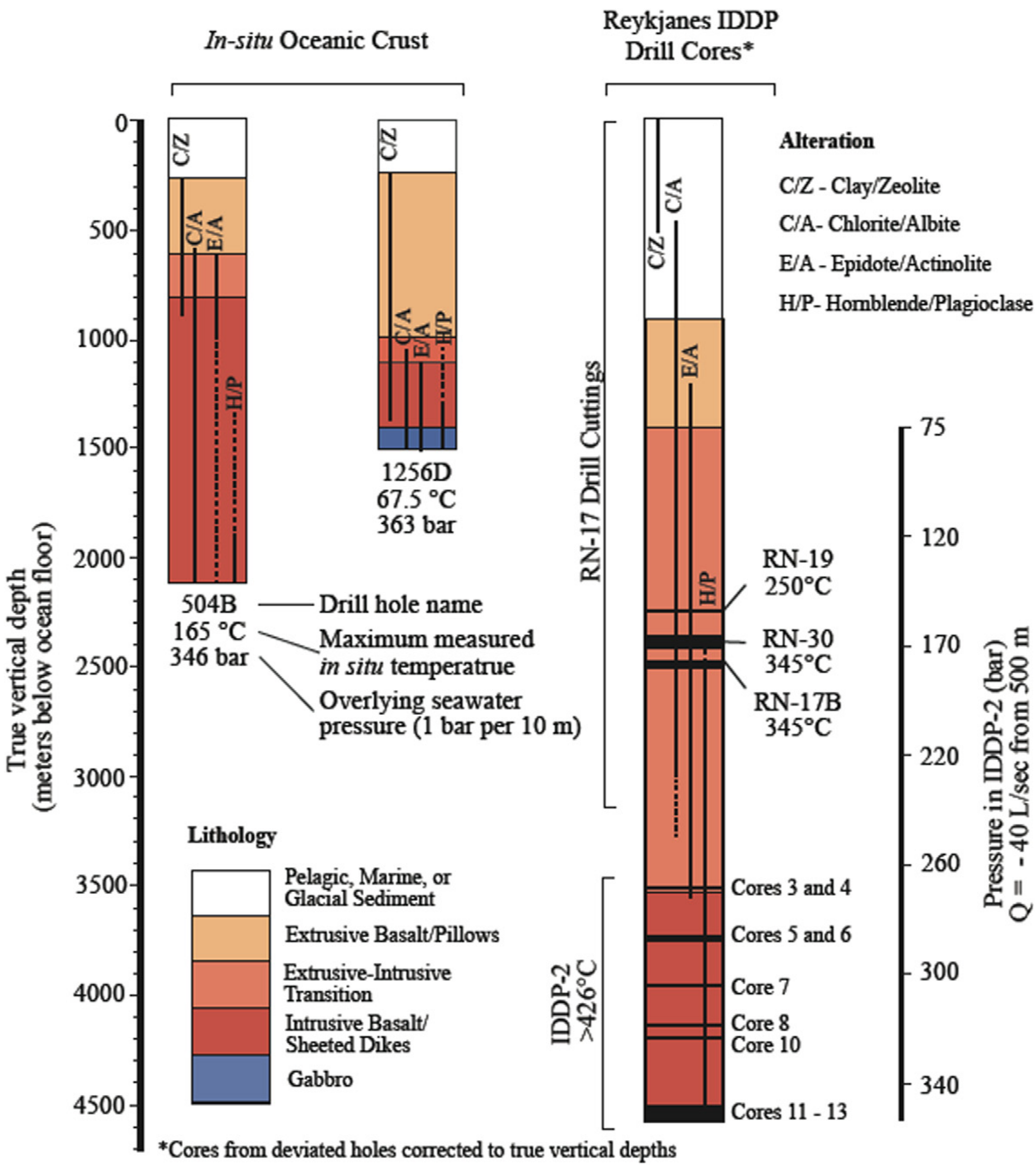

Fig. 15. Comparison of alteration and rock types observed in IDDP cores from the seawater-recharged Reykjanes geothermal system to the two deepest holes drilled into in situ oceanic crust (in Friðleifsson et al., 2017). The horizontal black lines in the IDDP core show the locations of cores recovered.

observed in the range of 200–400 °C. In hyaloclastite, temperature has no effect on permeability up to 800 °C.

Acoustic velocities (P-waves), measured up to 300 MPa using the time of flight method, display similar results: they increase non-linearly in dolerite up to 200 MPa, while they remain constant in hyaloclastites, showing a weak effect of pressure. P-waves velocities at 100 MPa of confining pressure are given in Table 2. Acoustic properties at high temperature are currently being investigated at the Geosciences Montpellier laboratory. Electrical conductivities were measured under dry and saturated conditions (Nono et al., 2017) to highlight the role of fluids on electrical conductivity up to supercritical conditions. Under saturated conditions, the electrical conductivities were measured at different fluid salinities, in order to mimic the variability of geothermal fluids and to investigate the respective contribution of pore fluid conductivity and interfacial conductivity due to fluid-rock electrical charge exchanges (electrical double layer). Results at typical P-T conditions of supercritical reservoirs are given in Table 2 for fluid of near sea-water salinities, like the Reykjanes geothermal reservoir fluids. The measurements at 400 °C highlight the clear differences between electrical conductivity of dry rocks and saturated rocks, saturated rocks being more conductive by one to two orders of magnitude relative to dry rocks. This indicates it may be possible to detect the electrical signature of supercritical fluids in the Icelandic crust. Under these conditions, it was found that surface conduction dominates the electrical conductivity of rock samples. Additional measurements will be performed on the IDDP-2 core samples, where electrical conductivity and permeability are still lacking. Specific behaviors, such as the increase of permeability in some dolerites due to thermal effects, as well as the role of surface contribution to conductivity and fluid-rock interaction at high temperature need more investigations to better characterize the physical properties of rocks at supercritical conditions.

Table 2
Mineralogical and petrophysical properties of mini-cores from different drill holes in Reykjanes Peninsula. Permeability and electrical properties are given at in-situ conditions corresponding to supercritical conditions. Electrical properties are given for samples saturated with a fluid of near sea-water salinity.

Sample (core number)	RN-19 (2)	RN-30 (1)	RN-17B (2)	RN-15-IDDP2 (12)
Depth (m)	2245	2510	2798	12 samples ranging from 3638 to 4654 m
Rock type	Dolerite	Dolerite	Hyaloclastite	Dolerites
In-situ T(°C)	320	350	350	350–450
Mineralogy from XRD (when content > 5%)	Augite, plagioclase chlorite	Plagioclase, augite, actinolite, chlorite	Epidote, albite, amphibole	Plagioclase (38–55%)–amphibole (20–50%)
Porosity (%) at room conditions (std. dev.)	2.9 (0,4)	3.3 (0,4)	13.4 (2.8)	1–3%
Permeability at $P_c = 100$ MPa and T = 400 °C and $P_f = 20$ MPa ($m^2.s^{-1}$)	$1.6–30 \times 10^{-19}$	$0.3–4.5 \times 10^{-19}$	1.6×10^{-16}	TBD
Dry electrical conductivity at $P_c = 100$ MPa & T = 400 °C ($S\ m^{-1}$)	10^{-4}	10^{-3}	$10^{-3.8}$	$10^{-3.8}$ S (sample PP2 at 4649,25 m)
Saturated electrical conductivity at $P_c = 100$ MPa, 5 = 400 °C and $P_f = 30$ MPa	0.057 ± 0,05	0.51 ± 0.05	0.2 ± 0.05	TBD
P-wave velocity at $P_c = 100$ MPa ($m\ s^{-1}$)	4900 ± 100	5863 ± 100	4900 ± 100	5060 ± 100

12. Discussion

12.1. Implications for mid-ocean ridge environments

The Reykjanes ridge is the portion of the Mid-Atlantic Ridge (MAR) that extends onshore in southwest Iceland, where the subaerial location of the Reykjanes Peninsula allows investigation of the deep structure of the volcanic/hydrothermal system of a slow spreading mid-ocean ridge. However, the enhanced magma productivity from the Iceland hotspot has produced thicker crust at the Reykjanes ridge than is typical for the Mid-Atlantic Ridge. Our understanding of the structure of oceanic crust is derived to a large extent by activities by the Deep Sea Drilling Program (DSDP)/Ocean Drilling Program (ODP)/Integrated Ocean Drilling Program (IODP), which have been largely focused on crust formed at intermediate to fast spreading rates. The deepest drill holes completed in in situ oceanic crust are Holes 504B and 1256D, near the fast spreading East Pacific Rise (Anderson et al., 1982; Alt et al., 1986; Bach et al., 2003; Alt et al., 2010). Studies of core from holes 504B and 1256D from near the East Pacific Rise can provide useful background to understand the rock types and alteration recorded by IDDP drill cores from the seawater-recharged and basalt-hosted Reykjanes geothermal field, and vice versa.

Consistent with a thicker crust at Reykjanes (~16 km; Bjarnason et al., 1993) as compared to that occurring at fast-spreading centers, the IDDP cores have confirmed that there is a greater thickness for the volcanic/sheeted dike transition than that occurring at fast-spreading centers, such as that observed in Holes 504B and 1256D (Fig. 15). Crustal age is another key difference between Reykjanes and rocks sampled in Holes 504B and 1256D. The crust at Reykjanes is actively forming and its rocks are certainly younger than 1 Ma, whereas Hole 504B and 1256D were completed in 5.9 and 15 Ma old crust and had maximum in situ temperatures of only 165 °C and 67.5 °C respectively (Becker et al., 1989; Teagle et al., 2006). The implication is that the older, colder rocks sampled in Holes 504B and 1256D have migrated away from the spreading center and have a longer and more complex record of integrated alteration-induced geochemical changes, including both higher temperatures near axial hydrothermal and lower-temperature off-axial processes. These characteristics are particularly useful for estimating bulk elemental fluxes between oceans and oceanic crust (e.g. Laverne et al., 2001; Bach et al., 2003). However, due to overprinting by subsequent low-temperature alteration processes, these off-axis processes obscure the high temperature alteration and geochemical exchange actively occurring in the hydrothermal root-zone at the ridge axis.

The IDDP drill cores therefore provide an unprecedented opportunity to investigate water-rock reactions occurring in the active roots of an analog of a submarine 'black smoker' hydrothermal system; one that is free of overprinting by lower-temperature alteration. Rocks at supercritical temperatures from an active hydrothermal environment have not previously been sampled. The IDDP-2 rock samples, and down hole data record supercritical conditions that lack adequate physical and thermodynamic data to be rigorously described using theoretical models. Initial studies reveal the deep hydrothermal system is a dynamic environment with more variability in physical and chemical conditions than simple conceptual models of an environment with fixed physical properties would predict. Despite low intrinsic permeability and modest amounts of fracturing, the rocks are pervasively altered, likely due to the properties of supercritical fluids such as low viscosity that facilitate extensive water/rock interaction.

Even under the extreme active hydrothermal P-T conditions deep in the IDDP-2, disequilibrium greenschist/amphibolite alteration assemblages occur over a large depth range as sampled in the RN-17B and in shallow IDDP-2 drill cores. We hypothesize that this may reflect prograde growth of the hydrothermal system, due to repeated dike intrusions and crustal subsidence that expand the P-T regime into the stability fields of minerals of the amphibolite and higher metamorphic facies. IDDP-2 rocks also have styles of alteration not previously predicted for hydrothermal root zones, e.g. the occurrence of hydrothermal biotite, that appears to be related to the occurrence of K-rich brine formed from phase separation (Zierenberg et al., 2017). Traces of this brine were captured in drill core pore space that are the focus of ongoing studies that may provide the first direct fluid samples that will allow us to characterize downhole fluids in the IDDP-2, an onshore analog of the root zone of a submarine black smoker.

12.2. Implications for the development of geothermal resources

As discussed above, the deep geological environment of the Reykjanes geothermal system is of great interest to the scientific community, situated as it is on the landward extension of the Mid Atlantic Ridge (Elders and Friðleifsson, 2010) and provides easier access to geochemical process occurring under seafloor spreading centers worldwide. However, in the future, the IDDP's demonstration that it is possible to drill into supercritical conditions could also have a large impact on improving the economics of high-temperature geothermal resources worldwide. The potential advantages of the approach of accessing hotter and deeper geothermal resources include: (1) Improvement in the ratio of drilling costs to power output per well. Although deeper wells would be more expensive, this should be offset by much higher power output per well. (2) Improvement in the power output of existing geothermal fields without increasing their environmental footprints. (3) Improvement in the lifetime of existing geothermal fields by increasing the size of the producible resource by extending it downwards. (4) Accessing a deeper, hotter, environment for fluid injection. (5) Improvement in the economics of geothermal power production. Higher-enthalpy aqueous working fluids in a turbine have a higher heat-to-power efficiency and therefore should potentially yield more favorable economics. Higher temperatures of the working fluid result in higher exergy (i.e., availability of maximum electrical power production potential for a given flow rate).

Recent numerical simulations of magma-heated, saline, hydrothermal systems indicate that the first-order control on the dynamics and efficiency of heat and mass transfer is phase separation near the intrusion (Scott et al., 2017). Above deep intrusions emplaced at >4 km depth, where fluid pressure is >30 MPa, phase separation occurs by condensation of hypersaline brine from a saline intermediate-density fluid. The fraction of brine remains small, and advective and vapor-dominated mass and heat fluxes are therefore maximized for exploitation of supercritical geothermal resources. Thus, the Reykjanes system, although saline, is an attractive target to test utilization of supercritical geothermal resources. If successful, the long-term flow tests now being planned for the IDDP-2, will supply useful information on the technology and economics of the production of useful energy from supercritical geothermal systems. Iceland is fortunate in having several likely sites for such developments. Planning for drilling the IDDP-3 well at Hellisheidi is already underway, and, subject to the availability of funding, drilling could begin as early as 2021–2022.

However, supercritical conditions are not restricted to Iceland, but should occur deep in any young volcanic-hosted geothermal system. Deep wells drilled in geothermal fields such as Kakkonda in NE Japan (Muraoka et al., 1998), Larderello in Italy (Bertini et al., 1980), Los Humeros in Mexico (Gutiérrez-Negrín and Izquierdo-Montalvo, 2010), and Salton Sea in USA (Kaspereit et al., 2016) have all encountered temperatures above 374 °C. Development of supercritical geothermal resources could be possible there and in many other volcanic areas worldwide. For example, in Japan the Japanese Beyond the Brittle Project (JBBP) is an ambitious EGS project to extract geothermal energy from >500 °C neogranites (Muraoka et al., 2014). Another possibility, when the technology and economics in the future permit, is to produce useful energy directly from the worldwide submarine mid-ocean ridge systems (Elders, 2015). Vents discharging supercritical water on the sea floor have been directly observed at 5° S on the Mid-Atlantic Ridge (Koshchinsky et al., 2008).

13. Summary and conclusions

The IDDP-2 is the deepest and hottest geothermal production well in Iceland and has demonstrated, for the first time, that it is possible to drill into supercritical conditions. The actual temperature in the formation is expected to exceed the measured 426 °C reported during drilling, and likely reach about 535 °C at 4.5 km depth. The well drilled through rocks like those of the mid-ocean spreading centers, but with a thicker section of sheeted dikes due to a greater input of basalt magma from the Icelandic hotspot. Fracture permeability exists even in the supercritical part of the well and has been enhanced by injecting cold water. Although the deeper rocks have very low porosity and sparse fractures, they are pervasively altered to amphibole- and pyroxene-bearing mineral assemblages, suggesting high fluid/rock ratios through the medium of low viscosity supercritical water. The uppermost part of a previously postulated aseismic body, from 3 to 5 km depth below the drill field, became seismically active during the deep drilling. A possible explanation for the previous lack of natural earthquakes in this body is that the body is at temperatures very close to the brittle-ductile boundary for normal strain rates, but injection of cold water during drilling induced fracturing. Drill cores obtained from the IDDP-2 permit, for the first time, investigation of high temperature alteration during the transition from magmatic to hydrothermal conditions and the physical behavior of such rocks under in-situ conditions. Intensive geophysical surveys of the Reykjanes peninsula area offer the opportunity of comparing small scale investigations to large scale geophysics, allowing for a better understanding of geophysical signals in terms of rocks properties and in situ conditions. Various scenarios have been suggested for the deep fluid chemistry of well IDDP-2, but the composition will remain unknown until flow tests allow fluid sampling and analysis. The next step is to allow the well to warm-up and perform flow tests and fluid sampling. Designing the wellhead equipment, flow line and preparation for flow testing is underway. If that step is successful, it will have significant technical and economic implications for the geothermal industry worldwide, wherever supercritical conditions exist at drillable depth.

Acknowledgements

The IDDP-2 was funded by HS Orka, Landsvirkjun, Orkuveita Reykjavíkur, and the National Energy Authority (Orkustofnun) in Iceland, together with Statoil (Equinor), the Norwegian Oil and Gas Company. The IDDP has also received funding from the EU H2020 (DEEPEGS, grant no. 690771). Funding for IDDP to obtain spot cores at Reykjanes and elsewhere was provided by ICDP and the US NSF (grant no. 05076725). EU FP7 project IMAGE (grant number No. 608553) supported petrophysical studies of cores. The authors also thank two anonymous reviewers for their contributions to the improvement of this paper.

References

Albertsson, A., Bjarnason, J.Ó., Gunnarsson, T., Ballzus, C., Ingason, K., 2003. Iceland Deep Drilling Project, feasibility report. In: Friðleifsson, G.Ó. (Ed.), Part III: Fluid Handling and Evaluation, 33 p. Orkustofnun Report OS-2003-007 (also at www.iddp.is).

Alt, J.C., Honnorez, J., Laverne, C., Emmerman, R., 1986. Hydrothermal alteration of a 1 km section through the upper oceanic crust, deep sea drilling project Hole 504B: mineralogy, chemistry, and evolution of seawater basalt intrusions. J. Geophys. Res. 91, 10,309–310,335.

Alt, J.C., Laverne, C., Coggon, R.M., Teagle, D.A.H., Banerjee, N.R., Morgan, S., Smith-Duque, C.E., Harris, M., Galli, L., 2010. Subsurface structure of a submarine hydrothermal system in ocean crust formed at the East Pacific Rise, ODP/IODP Site 1256. Geochem. Geophys. Geosyst. 11 (n/a-n/a).

Anderson, R.N., Honnorez, J., Becker, K., Adamson, A.C., Alt, J.C., Emmerman, R., Kempton, P.D., Kinoshita, H., Laverne, C., Mottl, M.J., Newmarks, R.L., 1982. Hole 504B, the first reference section over 1 km through Layer 2 of the oceanic crust. Nature 300, 589–594.

Ármannsson, H., Friðriksson, Þ., Guðfinnsson, G.H., Ólafsson, M., Óskarsson, F., Þorbjörnsson, D., 2014. IDDP-The chemistry of the IDDP-01 well fluids in relation to the geochemistry of the Krafla geothermal system. Geothermics 49, 66–75.

Arnórsson, S., 1978. Major element chemistry of the geothermal sea-water at Reykjanes and Svartsengi, Iceland. Mineral. Mag. 42, 209–220.

Arnórsson, S., Andrésdóttir, A., 1995. Processes controlling the distribution of boron and chlorine in natural waters in Iceland. Geochim. Cosmochim. Acta 59, 4125–4146.

Axelsson, G., Arnaldsson, A., Berthet, J.C., Bromley, C.J., Guðnason, E.Á., Hreinsdóttir, S., Karlsdóttir, R., Magnússon, I.Þ., Michalczewska, K.L., Sigmundsson, F., Sigurðsson, Ó., 2015. Renewability assessment of the Reykjanes Geothermal System, SW Iceland. Proceedings of the 2015 World Geothermal Congress, Melbourne, Australia, 19–25 April 2015, Paper 16008.

Bach, W., Peucker-Ehrenbrink, B., Hart, S.R., Blusztajn, J.S., 2003. Geochemistry of hydrothermally altered oceanic crust: DSDP/ODP Hole 504B - implications for seawater-crust exchange budgets and Sr- and Pb-isotopic evolution of the mantle. Geochem. Geophys. Geosyst. 4, 1–29.

Becker, K., Sakai, H., Adamson, A.C., Alexandrovich, J., Alt, J.C., Anderson, R.N., Bideau, D., Gable, R., Herzig, P.M., Houghton, S., Ishizuka, H., Kawahata, H., Kinoshita, H., Langseth, M.G., Lovell, M.A., Malpas, J., Masuda, H., Merrill, R.B., Morin, R.H., Mottl, M.J., Pariso, J.E., Pezard, P., Phillips, J., Sparks, J., Uhlig, S., 1989. Drilling deep into young oceanic crust, hole 504B, Costa Rica Rift. Rev. Geophys. 27, 79–102.

Bertini, G., Giovannoni, A., Stefani, G.C., Gianelli, G., Puxeddu, M., Squarci, P., 1980. Deep exploration in Larderello Field: Sasso 22 drilling venture advances in European geothermal research. In: Strub, A.S., Ungemach, P. (Eds.), Proceedings of the Second International Seminar on the Results of EC Geothermal Energy Research. Springer Netherlands, pp. 303–311.

Bischoff, J.L., Rosenbauer, R.J., 1988. Liquid-vapor relations in the critical region of the system NaCl-H_2O from 380 °C to 414 °C: a refined determination of the critical point of seawater. Geochim. Cosmochim. Acta 52, 2121–2126.

Bjarnason, J.Ö., 1995. Chemical composition of freshwater, saltwater and seawater in the Reykjanes Area, Southwest Iceland. Orkustofnun, Geothermal Division, Short Report JÖB-95-04 (3p).

Bjarnason, I.Th., Menke, W., Flóvenz, Ó.G., Caress, D., 1993. Tomographic Image of the Mid-Atlantic Plate Boundary. J. Geophys. Res. 98 (B4), 6607–6622.

Björnsson, S., Arnórsson, S., Tómasson, J., 1972. Economic evaluation of Reykjanes thermal brine area. Am. Assoc. Pet. Geol. Bull. 56 (12), 2380–2391.

Coumou, D., Driesner, T., Weis, P., Heinrich, C.A., 2009. Phase separation, brine formation, and salinity variation at Black Smoker hydrothermal systems. J. Geophys. Res. 114, 1–16.

Dunn, J.C., Hardee, H.C., 1981. Superconvecting geothermal zones. J. Volcanol. Geotherm. Res. 11, 189–201.

Elders, W.A., 2015. The potential for on- and off-shore high-enthalpy geothermal systems in the USA. Proceedings of the Fortieth Workshop on Geothermal Reservoir Engineering, Stanford University, January 26–28, 2015, Paper SGP-TR-204, pp. 1–6.

Elders, W.A., Friðleifsson, G.Ó., 2010. Implications of the Iceland Deep Drilling Project for improving understanding of hydrothermal processes at slow spreading mid-ocean ridges. In: Rona, P.A., Devey, C.W., Dyment, J., Murton, B.J. (Eds.), Diversity of Hydrothermal Systems on Slow Spreading Ocean Ridges. vol. 188. American Geophysical Union, Geophysical Monograph, pp. 91–112.

Elders, W.A., Friðleifsson, G.Ó., Saito, S., 2001. The Iceland Deep Drilling Project: a search for supercritical fluids. Trans. Geothermal Resources Council 21, 297–300.

Elders, W.A., Friðleifsson, G.Ó., Zierenberg, R.A., Pope, E.C., Mortensen, A.K., Guðmundsson, Á., Lowenstern, J.B., Marks, N.E., Owens, L., Bird, D.K., Reed, M., Olsen, N.J., Schiffman, P., 2011. Origin of a rhyolite that intruded a geothermal well while drilling in a basaltic volcano, at Krafla, Iceland. Geology 39 (3), 231–234.

Escobedo, D., Gibert, B., Parat, F., Loggia, D., Levy, L., Fridleifsson, G.O., Zierenberg, R.A., 2017. Petrophysical and mineralogical characterization of IDDP-2 mini-core samples from depths of 3650 to 4650 m. IMAGE Final conference, Akureyri.

Fournier, R.O., 1999. Hydrothermal processes related to movement of fluid from plastic into brittle rock in the magmatic-epithermal environment. Econ. Geol. 94 (8), 1193–1211.

Fournier, R.O., 2007. Hydrothermal systems and volcano geochemistry. In: Durzin, D. (Ed.), Volcano Deformation: Geodetic Monitoring Techniques. Springer-Praxis, Berlin, New York, Chichester, UK, pp. 323–341 (Chapter 10).

Fowler, A.P.G., Zierenberg, R.A., 2016a. Geochemical bias in drill cutting samples versus drill core samples returned from the Reykjanes Geothermal System, Iceland. Geothermics 62, 48–60.

Fowler, A.P.G., Zierenberg, R.A., 2016b. Elemental changes and alteration recorded by basaltic drill core samples recovered from in-situ temperatures up to 345 °C in the active, seawater-recharged Reykjanes Geothermal System, Iceland. Geochem. Geophys. Geosyst. 17.

Fowler, A.P.G., Zierenberg, R.A., Schiffman, P., Marks, N., Friðleifsson, G.Ó., 2015. Evolution of fluid–rock interaction in the Reykjanes Geothermal System, Iceland: evidence from Iceland Deep Drilling Project core RN-17B. J. Volcanol. Geotherm. Res. 302, 47–63.

Franzson, H., Thórdarson, S., Björnsson, G., Guðlaugsson, S.Þ., Richter, B., Friðleifsson, G.Ó., Þórhallsson, S., 2002. Reykjanes high-temperature field, SW-Iceland. Geology and hydrothermal alteration of well RN-10. Proceedings of the 27th Workshop on Geothermal Reservoir Engineering, Stanford University, California, January 28–30 2002, SGP-TR-171.

Friðleifsson, G.Ó., Albertsson, A., 2000. Deep geothermal drilling at Reykjanes Ridge: opportunity for an international collaboration. Proceedings of the World Geothermal Congress, Kyushu-Tohoku, Japan, May 28–June 10, 2000, pp. 3701–3706.

Fridleifsson, G.O., Elders, W.A., 2005. The Iceland Deep Drilling Project: a search for deep unconventional geothermal resources. Geothermics 34, 269–285.

Friðleifsson, G.Ó., Elders, W.A., 2017. Successful drilling for supercritical geothermal resources at Reykjanes in SW Iceland. GRC Transactions. vol. 41, pp. 1095–1107.

Friðleifsson, G.Ó., Richter, B., 2010. The geological significance of two IDDP-ICDP spot cores from the Reykjanes geothermal field, Iceland. Proceedings World Geothermal Congress 2010 Bali, Indonesia, 25–29 April 2010, pp. 1–7.

Friðleifsson, G.Ó., Ármannsson, H., Árnason, K., Bjarnason, I.Þ., Gíslason, G., 2003. Iceland Deep Drilling Project, feasibility report. In: Friðleifsson, G.Ó. (Ed.), Part I: Geosciences and Site Selection, Orkustofnun Report OS-2003-007, 104 p (also at www.idddp.is).

Friðleifsson, G.O., Blischke, A., Reyr, B.K., Richter, B., Einarsson, G.M., Jónasson, H., Franzson, H., Sigurðsson, Ó., Danielsen, P.E., Jónsson, S.S., Thordarson, S., Þórhallsson, S., Harðardóttir, V., Egilsson, T., 2005. Reykjanes Well Report RN-17 and RN-17ST, ISOR-2005/007. Iceland Geosurvey, Reykjavik.

Friðleifsson, G.Ó., Sigurdsson, Ó., Þorbjörnsson, D., Karlsdóttir, R., Gíslason, Þ., Albertsson, A., Elders, W.A., 2014. Preparation for drilling well IDDP-2 at Reykjanes. Geothermics 49, 119–126.

Friðleifsson, G.Ó., Elders, W.A., Zierenberg, R.A., Stefánsson, A., Fowler, A.P.G., Weisenberger, T.B., Harðarson, B.S., Mesfin, K.G., 2017. The Iceland Deep Drilling Project 4.5 km deep well, IDDP-2, in the sea-water recharged Reykjanes geothermal field in SW Iceland has successful reached its supercritical target. Sci. Drill. 23, 1–12.

Friðriksson, Þ., Stefánsson, A., Óskarsson, F., Eyjólfsdóttir, E., Sigurðsson, Ó., 2015. Fluid chemistry scenarios anticipated for IDDP-2 to be drilled in Reykjanes, Iceland. Proceedings of the 2015 World Geothermal Congress, Melbourne, Australia, 19–25 April 2015, Paper 14068.

Gee, M.A.M., Thirlwall, M.F., Taylor, R.N., Lowry, D., Murton, B.J., 1998. Crustal processes: Major controls on Reykjanes Peninsula lava chemistry, SW Iceland. J. Petrol. 39, 819–839.

Guðnason, E.Á., Ágústsson, K., Gunnarsson, K., Flóvenz, Ó.G., 2015. Seismic activity on Reykjanes December 2014–November 2015. Iceland GeoSurvey, ÍSOR-2015/068 (31 pp).

Guðnason, E.Á., Ágústsson, K., Gunnarsson, K., 2016. Seismic activity on Reykjanes December 2015–November 2016. Iceland GeoSurvey, ÍSOR-2016/090 (45 pp).

Gutiérrez-Negrín, L.C.A., Izquierdo-Montalvo, G., 2010. Review and update of the main features of the Los Humeros geothermal field, Mexico. Proc. World Geotherm. Congr., Bali Indonesia 25–29 April 2010, pp. 1–5.

Harðardóttir, H., Hannington, M., Hedenquist, J., Kjarsgaard, I., Hoal, K., 2012. Cu-rich scales in the Reykjanes geothermal system. Econ. Geol. 105, 1143–1155.

Harðardóttir, V., Hannington, M., Hedenquist, J., 2013. Metal concentrations and metal deposition in deep geothermal wells at the Reykjanes high-temperature area, Iceland. Procedia Earth and Planetary Science 7, 338–341.

Hashida, T., Bignall, G., Tsuchiya, N., Takahashi, T., Tanifuji, K., 2001. Fracture Generation and water rock interaction processes in supercritical deep seated geothermal reservoirs. Geothermal Resources Council Transactions 25, 225–229.

Helgadóttir, H.M., Gunnarsdóttir, S.H., Guðfinnsson, G.H., Ingólfsson, H., 2009. Reykjanes-Hola RN-17b. Borun vinnsluhluta frá 933 m í 3077 m dýpi. ISOR-2009/008, 58 pp and Two Appendices, on Daily Reports and Coring Report 96 p and 15 p.

Hokstad, K., Tänavsuu-Milkeviciene, K., 2017. Temperature Prediction by Multigeophysical Inversion: application to the IDDP-2 Well at Reykjanes, Iceland. GRC Transactions 41, 1141–1152.

Horner, D.R., 1951. Pressure build up in wells. 3d World Petroleum Congress, Hague, Netherlands, pp. 25–43.

Jakobsson, S.P., Jónsson, J., Shido, F., 1978. Petrology of the western Reykjanes Peninsula, Iceland. J. Petrol. 19 (4), 669–705.

Jónsson, S.S., Sigurgeirsson, M.Á., Sigurðsson, Ó., Ingólfsson, H., 2010. Reykjanes – Hola RN-15. 3. áfangi: Borun vinnsluhluta frá 804 m í 2507 m dýpi. Iceland GeoSurvey, ÍSOR-2010/050 (67 pp).

Karlsdóttir, R., Árnason, K., Vilhjálmsson, A.M., 2012. Reykjanes Geothermal Area, Southwest Iceland. 3D inversion of MT and TEM data. Iceland Geosurvey, ÍSOR-2012/059.

Kaspereit, D., Mann, M., Sanyal, S., Rickard, B., Osborn, W., Hulen, J., 2016. Updated conceptual model and reserve estimate for the Salton Sea geothermal field, Imperial Valley, California. Geothermal Resources Council Transactions. 40 (11).

Koshchinsky, A., Garbe-Schonberg, D., Sander, S., Schmidt, K., Gennerich, H.-H., Strauss, H., 2008. Hydrothermal venting at pressure-temperature conditions above the critical point of seawater, 5° S on the Mid-Atlantic Ridge. Geology 30 (8), 615–618.

Kristinsdóttir, L.H., Flóvenz, O.G., Árnason, K., Bruhn, D., Milsch, H., Spangenberg, E., Kulenkampff, J., 2010. Electrical conductivity and P-wave velocity in rock samples from high-temperature Icelandic geothermal fields. Geothermics 39 (1), 94–105.

Kristmannsdóttir, H., 1979. Alteration of basaltic rocks by hydrothermal activity at 100–300 °C. In: Mortland, Farmer (Eds.), Proceedings of the VI International Clay Conference 1978. Elsevier Sci. Pub. Comp, Amsterdam, pp. 359–367.

Kummerow, J., Raab, S., 2015. Temperature dependence of electrical resistivity – part II: a new experimental set-up to study fluid-saturated rocks. Energy Procedia 76, 247–255.

Laverne, C., Agrinier, P., Hermitte, D., Bohn, M., 2001. Chemical fluxes during hydrothermal alteration of a 1200-m long section of dikes in the oceanic crust, DSDP/ODP hole 504B. Chem. Geol. 181, 73–98.

Lonker, S.W., Franzson, H., Kristmannsdottir, H., 1993. Mineral fluid interactions in the Reykjanes and Svartsengi geothermal systems. Am. J. Sci. 293, 605–670.

Marks, N., Schiffman, P., Zierenberg, R., Franzson, H., Friðleifsson, G.Ó., 2010. Hydrothermal alteration in the Reykjanes geothermal system: insights from Iceland deep drilling program well RN-17. J. Volcanol. Geotherm. Res. 189, 172–190.

Marks, N., Schiffman, P., Zierenberg, R.A., 2011. High-grade contact metamorphism in the Reykjanes geothermal system: Implications for fluid-rock interactions at mid-oceanic ridge spreading centers. Geochem. Geophys. Geosyst. 12.

Marks, N., Zierenberg, R.A., Schiffman, P., 2015. Strontium and oxygen isotopic profiles through 3 km of hydrothermally altered oceanic crust in the Reykjanes Geothermal System, Iceland. Chem. Geol. 412, 34–47.

Mortensen, A.K., Guðmundsson, Á., Richter, B., Sigurðsson, Ó., Friðleifsson, G.Ó., Franzson, H., Jónsson, S.S., Danielssen, P.K., Ásmundsson, R.K., Thordarson, S., Egilsson, Þ., Skarphéðinsson, K., Þórisson, S., 2006. Well report for RN-19. Icelandic Geosurvey Report ISOR-2006/025, 59 p and Two Appendices (80 p), Daily Reports (in Icelandic) and a Coring Report (in English).

Muraoka, H., Uchida, T., Sasada, M., Yasukawa, K., Miyazaki, S.I., Doi, N., Saito, S., Sato, K., Tanaka, S., 1998. Deep geothermal resources survey program: Igneous, metamorphic and hydrothermal processes in a well encountering 500 C at 3729 m depth, Kakkonda, Japan. Geothermics 27, 507–534.

Muraoka, H., Asanuma, H., Tsuchiya, N., Ito, T., the participants of the ICDP/JBBP Workshop: The Japan Beyond-Brittle Project, 2014. Sci. Drill. 17, 51–59.

Nono, F., Gibert, B., Cichy, S.B., Loggia, D., Parat, F., Mainprice, D., 2016a. Electrical Conductivity of Icelandic Deep Geothermal Reservoirs: Insight from HT-HP Laboratory Experiments. EGU General assembly, Vienna.

Nono, F., Gibert, B., Cichy, S.B., Loggia, D., Parat, F., Mainprice, D., Azais, P., 2016b. Permeability of Icelandic Deep Geothermal Reservoirs: Insight from HP and HT Measurements. EGU General Assembly, Vienna.

Nono, F., Gibert, B., Loggia, D., Parat, F., Cichy, S.B., Violay, M., 2017. The Electrical conductivity of Icelandic deep geothermal reservoirs: insight from laboratory experiments. Submitted to JVGR.

Óskarsson, F., Gałeczka, I.M., 2017. Reykjanes production field. Geochemical monitoring in 2016. Iceland GeoSurvey, Report ÍSOR-2017/020.

Óskarsson, F., Friðriksson, Þ., Þorbjörnsson, D., 2015a. Geochemical monitoring of the Reykjanes geothermal reservoir 2003 to 2013. Proceedings of the 2015 World Geothermal Congress, Melbourne, Australia, 19–25 April 2015, Paper 14085.

Óskarsson, F., Inguaggiato, S., Friðriksson, Þ., Caliro, S., 2015b. Gas isotope characterization of the Reykjanes geothermal field, Iceland. Proceedings of the 2015 World Geothermal Congress, Melbourne, Australia, 19–25 April 2015, Paper 14018.

Palgan, D., Devey, C.W., Yeo, I.D., 2017. Volcanism and hydrothermalism on a hotspot–influenced ridge: comparing Reykjanes Peninsula and Reykjanes Ridge, Iceland. J. Volcanol. Geotherm. Res. 348, 62–81.

Pope, E.C., Bird, D.K., Arnórsson, S., Friðriksson, Þ., Elders, W.A., Friðleifsson, G.Ó., 2009. Isotopic constraints on ice age fluids in active geothermal systems: Reykjanes, Iceland. Geochim. Cosmochim. Acta 73, 4468–4488.

Saemundsson, Sigurgeirsson, M.Á., Friðleifsson, G.Ó., 2018. Geology and structure of Reykjanes. JVGR 2018 (this volume).

Schiffman, P., Friðleifsson, G.Ó., 1991. The smectite-chlorite transition in drillhole N 1-15, Nesjavellir geothermal field, Iceland - XRD, BSE and electron microprobe investigations. J. Metamorph. Geol. 9, 679–696.

Schiffman, P., Zierenberg, R.A., Mortensen, A.K., Friðleifsson, G.Ó., Elders, W.A., 2014. High temperature metamorphism in the conductive boundary layer adjacent to a rhyolite intrusion in the Krafla geothermal system, Iceland. Geothermics 49, 42–48.

Scott, S., Driesner, T., Weis, P., 2017. Boiling and condensation of saline geothermal fluids above magmatic intrusions. Geophys. Res. Lett. 44. https://doi.org/10.1002/2016GL071891.

Shanks III, W.C., 2001. Stable isotopes in seafloor hydrothermal systems: vent fluid, hydrothermal deposits, hydrothermal alteration, and microbial processes. In: Valley, J.W., Cole, D.R. (Eds.), Reviews in Mineralogy and Geochemistry. vol. 43, pp. 469–525.

Sigurgeirsson, M.Á., Ingólfsson, H., Harðarsson, B.S., Guðfinnsson, G.H., 2011. Reykjanes - well RN-30, drilling of well RN-30 from surface down to 2869 m. ÍSOR-2011/043, 83 p, and Appendix (156 p): Daily Reports Including Core Discussion.

Stefánsson, A., Gíslason, Þ., Sigurðsson, Ó., Friðleifsson, G.Ó., 2017. The drilling of RN-15/IDDP-2 research well at Reykjanes in SW Iceland. GRC Transactions. vol. 41, pp. 512–522.

Teagle, D.A.H., Alt, J.C., Umino, S., Miyashita, S., Banerjee, N.R., Wilson, D.S., the Expedition 309/312 Scientists, 2006. Expedition 309/312 summary. Proceedings of the Integrated Ocean Drilling Program 309/312, pp. 1–127.

Tester, J.W. (Ed.), 2006. The future of geothermal energy: impact of enhanced geothermal energy (EGS) on the United States in the 21st century. MIT Panel Report to the US Department of Energy, pp. 1–54 (Also at http://geothermal.inel.gov, DOI May 2112).

Thórhallsson, S., Matthíasson, M., Gíslason, Th., Ingason, K., Pálsson, B., Friðleifsson, G.Ó., 2003. Iceland Deep Drilling Project, feasibility report. In: Friðleifsson, G.Ó. (Ed.), Part II: Drilling Technology, Orkustofnun Report OS-2003-007, 75 p. & Appendix (45 p.) (also at www.iddp.is).

Tomasson, J., Kristmannsdottir, H., 1972. High temperature alteration minerals and thermal brines, Reykjanes, Iceland. Contrib. Mineral. Petrol. 36, 123–134.

Vadon, H., Sigmundsson, F., 1997. Crustal deformation from 1992 to 1995 at the Mid-Atlantic Ridge, Southwest Iceland, mapped by satellite radar interferometry. Science 275, 193–197.

Weisenberger, T.B., Harðarson, B.S., Kästner, F., Gunnarsdóttir, S.H., Tulinius, H., Guðmundsdóttir, V., Einarsson, G.M., Pétursson, F., Vilhjálmsson, S., Stefánsson, H.Ö., Níelsson, S., 2017. Well report – RN-15/IDDP-2. Drilling in Reykjanes – Phase 4 and 5 from 3000 to 4659. ISOR 2017/016 (277 p).

Yano, Y., Ishido, T., 1998. Numerical investigation of production behavior of deep geothermal reservoirs at super-critical conditions. Geothermics 27 (5/6), 705–721.

Zierenberg, R.A., Schiffman, P., Barfod, G.H., Lesher, C.E., Marks, N.E., Lowenstern, J.B., Mortensen, A.K., Pope, E.C., Bird, D.K., Reed, M.H., Friðleifsson, G.Ó., Elders, W.A., 2012. Composition and origin of rhyolite melt intersected by drilling in the Krafla geothermal field, Iceland. Contrib. Mineral. Petrol. 165 (2), 327–347.

Zierenberg, R.A., Fowler, A.P.G., Friðleifsson, G.Ó., Elders, W.A., Weisenberger, T.B., 2017. Preliminary description of rocks and alteration in IDDP-2 drill core samples recovered from the Reykjanes Geothermal System, Iceland. GRC Transact. 41, 1599–1615.